# Multiscale physics of nuclei from first principles

Gaute Hagen

Oak Ridge National Laboratory

SSNET'24: International Conference on Shapes and Symmetries in NUCLEI:
From Experiment to Theory

Orsay, November 7th, 2024
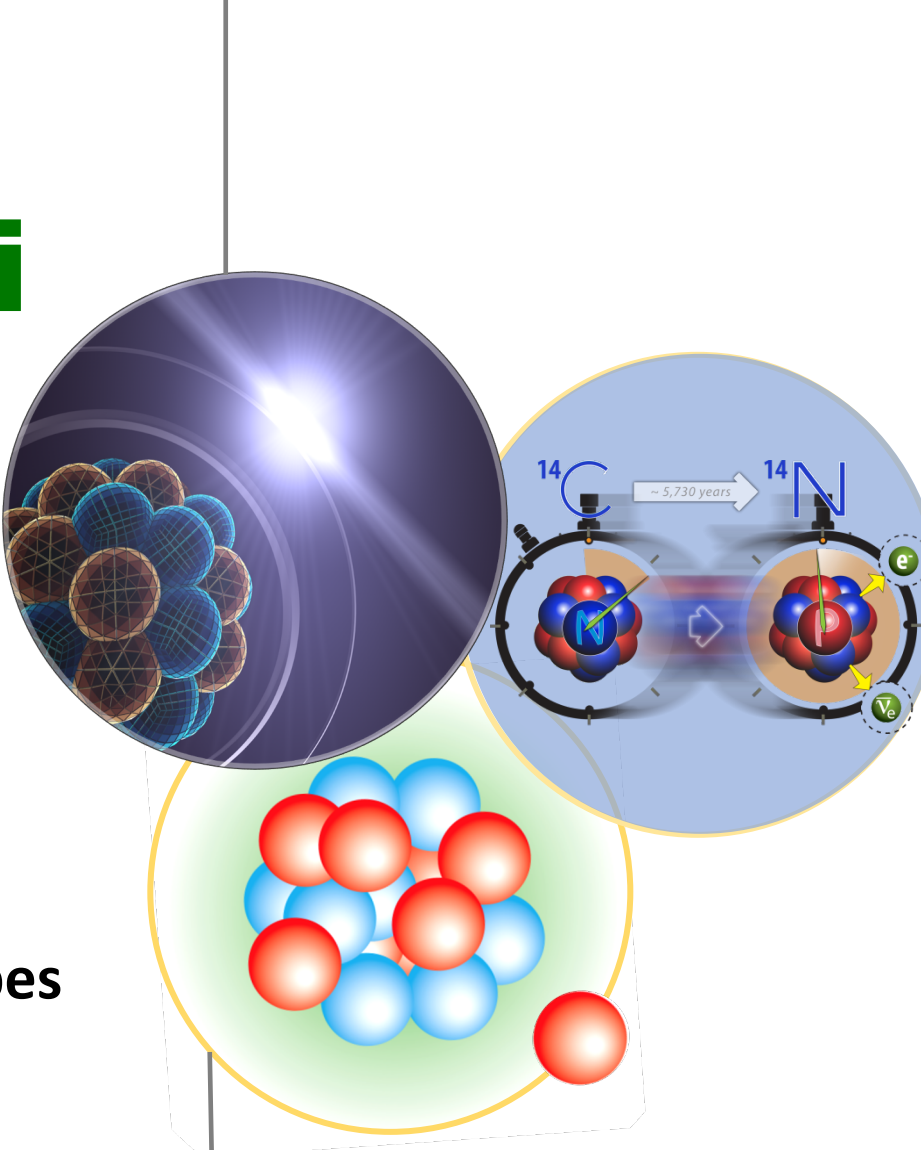
Collaborators

Tor Djärv (ORNL)

G. R. Jansen (ORNL)

T. Papenbrock (ORNL/UTK)

Zhonghao Sun (LSU)
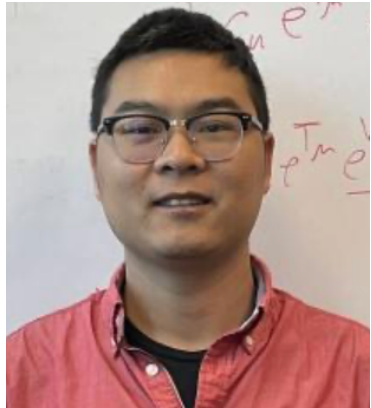
**Baishan Hu (Texas A&M)**
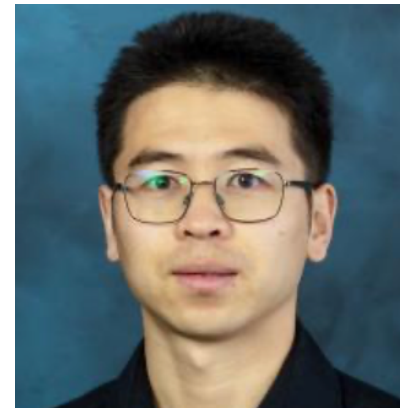
C. Forssén (Chalmers)

A. Ekström (Chalmers)

# Trend in realistic ab-initio calculations

- Tremendous progress in recent years because of ideas from EFT and the renormalization group
- Computational methods with polynomial cost (coupled clusters 🙂 quantum computing 🤔)
- Ever-increasing computer power?

Development with time (top500.org)

No. 1 in 2024

^{208}Pb (this work)

^{132}Sn 2020

^{100}Sn 2018

^{78}Ni 2016
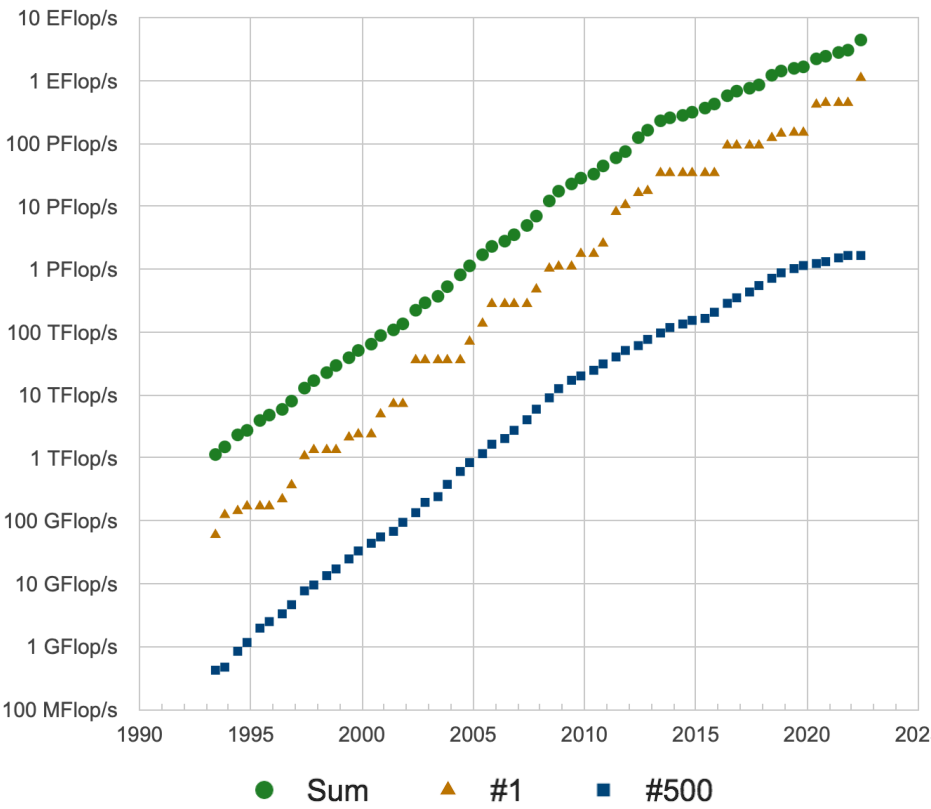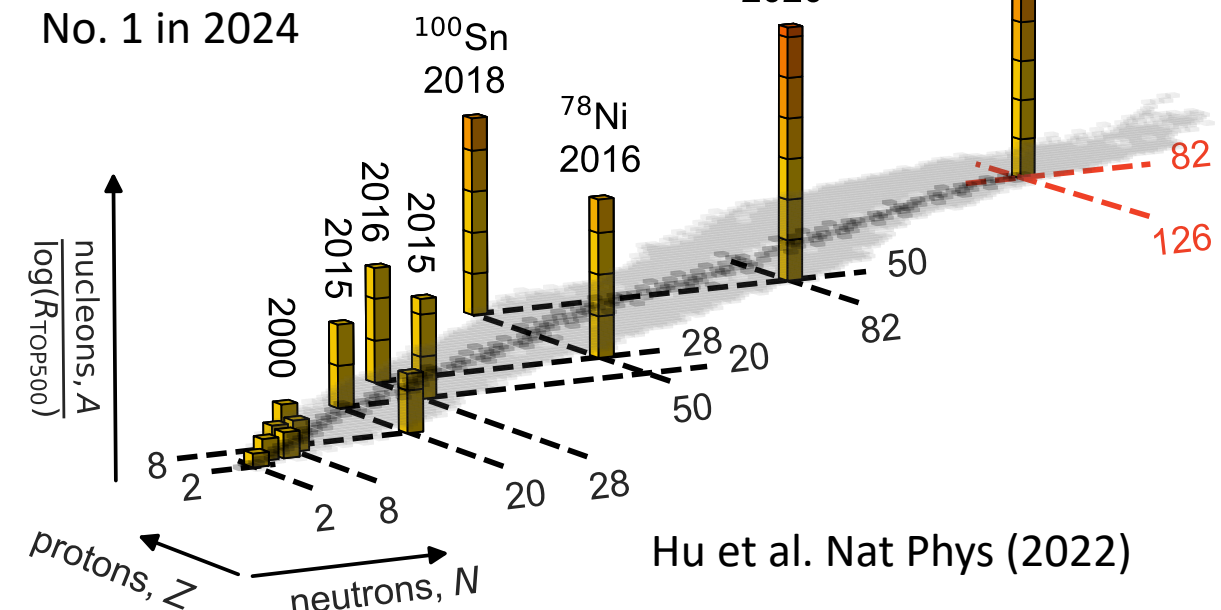
Hu et al. Nat Phys (2022)

Multiscale physics of nuclei from ab-initio methods

Degrees of Freedom — Energy (MeV)

- quarks, gluons
- constituent quarks — 940 neutron mass
- baryons, mesons — 140 pion mass
- protons, neutrons — 8 proton separation energy in lead
- nucleonic densities and currents — 1.12 vibrational state in tin
- collective coordinates — 0.043 rotational state in uranium

chiral effective field theory
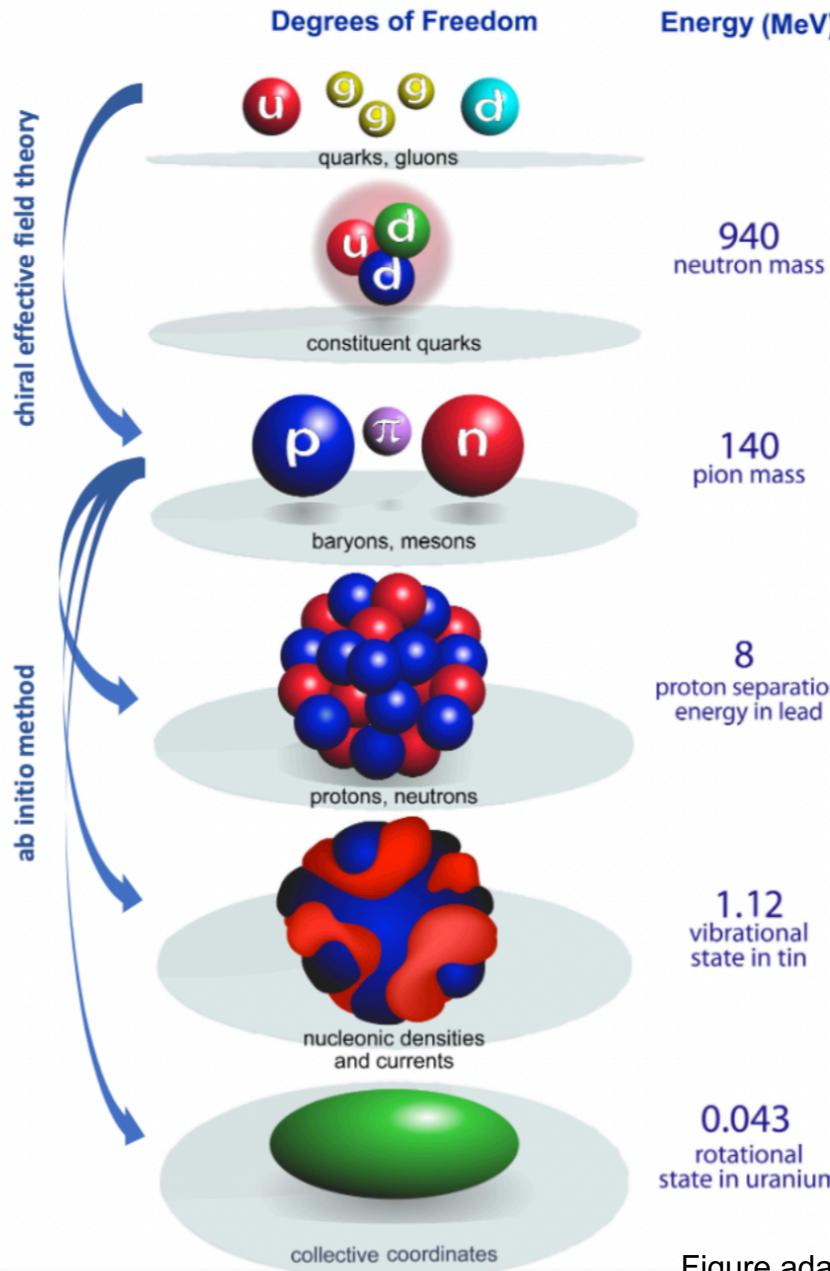
ab initio method

What is ab initio in nuclear theory?
A. Ekström et al, Frontiers (2023)

"we interpret the ab initio method to be a systematically improvable approach for quantitatively describing nuclei using the finest resolution scale possible while maximizing its predictive capabilities"

- Nuclei exhibit multiple energy scales ranging from hundreds of MeV in binding energies to fractions of an MeV for low-lying collective excitations.
- Describing these different energy scales within a unified ab-initio framework from chiral interactions is a long-standing challenge

Figure adapted from Bertsch, Dean, Nazarewicz, SciDAC review (2007)

Interactions from chiral effective field theory

Figure adapted from Bertsch, Dean, Nazarewicz, SciDAC review (2007)
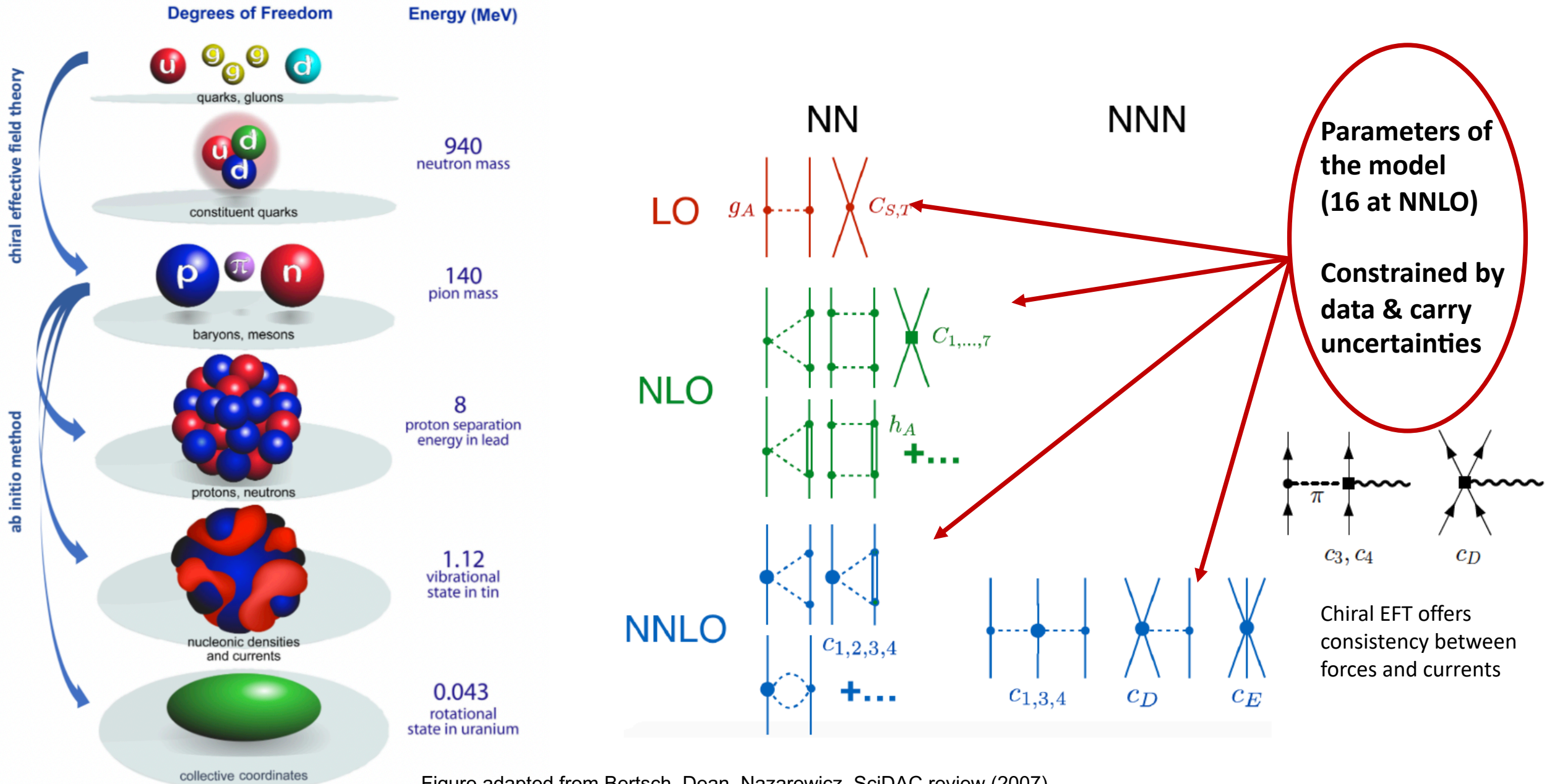
# Solving the quantum many-nucleon problem

An exponentially hard problem to solve!

$$H|\Psi\rangle = E|\Psi\rangle$$

1.1 exaflops

IBM Q Experience

Polynomial scaling

Systematically improvable approaches
with controlled approximations:
Coupled-cluster, IMSRG, Gorkov, SCGF,…

Emulators?
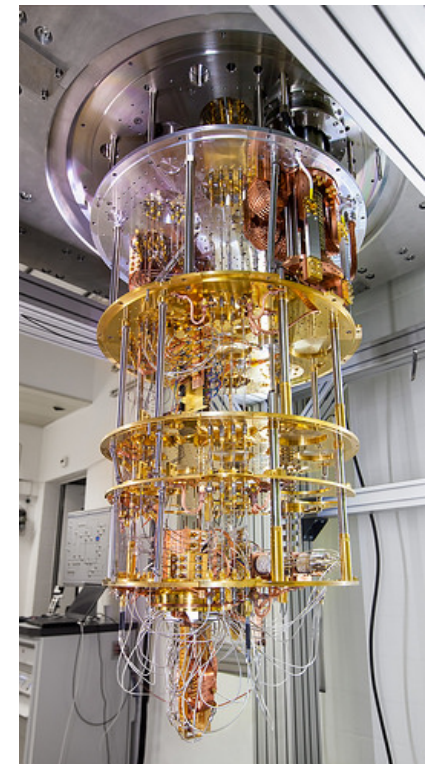
Fault tolerant quantum computing??

What precision/accuracy can we aim for in ab-initio modeling of nuclei?

Different many-body approaches agree with each for binding energies and radii
(challenges exist for transitions, isotope shifts, and deformed shapes)

H. Hergert Front. Phys., (2020)
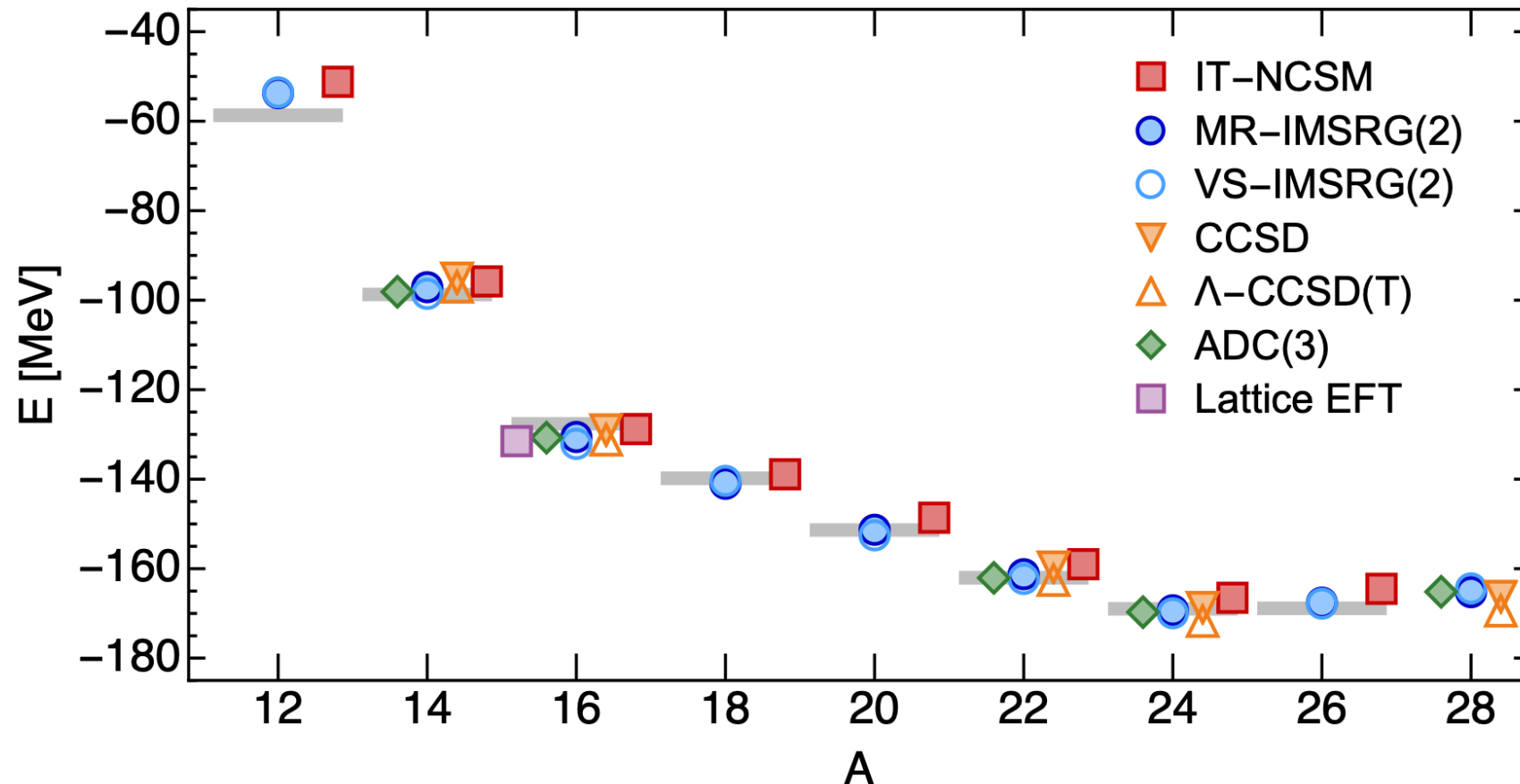
Coupled-cluster computations of deformed nuclei

- Compute Hartree-Fock reference state:

$$H = T - T_{\mathrm{CoM}} + V_{\mathrm{NN}} + \boxed{V_{\mathrm{3N}}}$$

$$W_0 + W_1 + W_2 + \cancel{W_3}$$

- Informs us about emergent breaking of symmetries

$$|\Psi\rangle = \Omega|\Phi\rangle$$
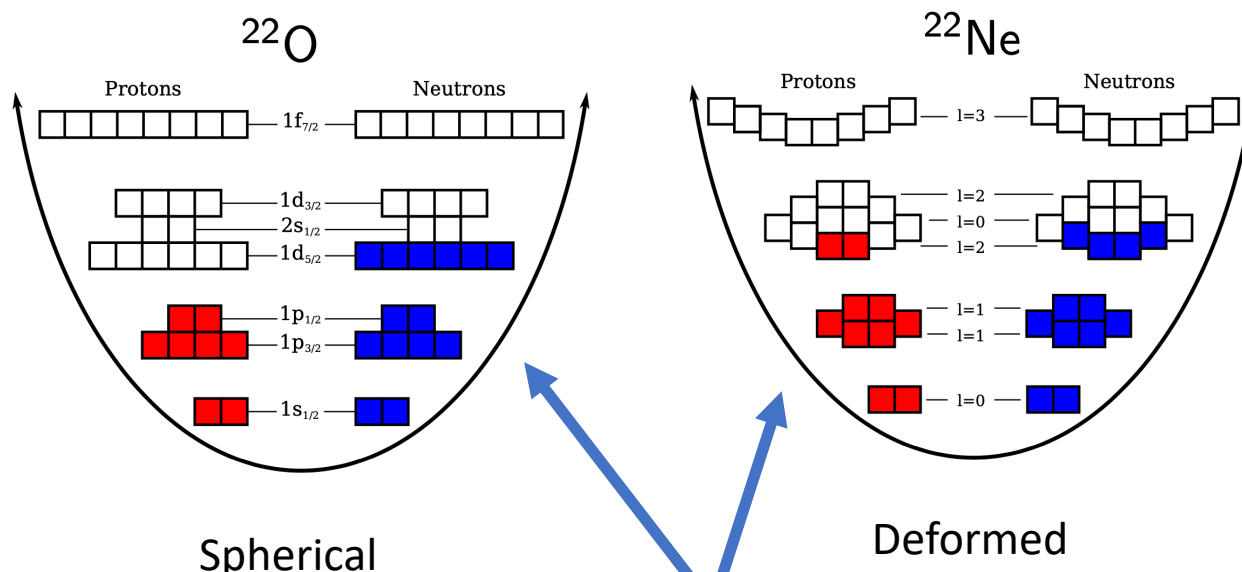
Wave-operator (includes many-body correlations)
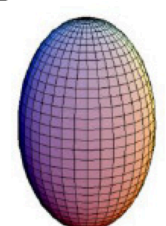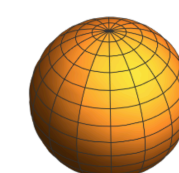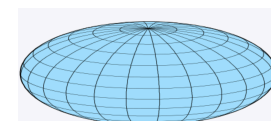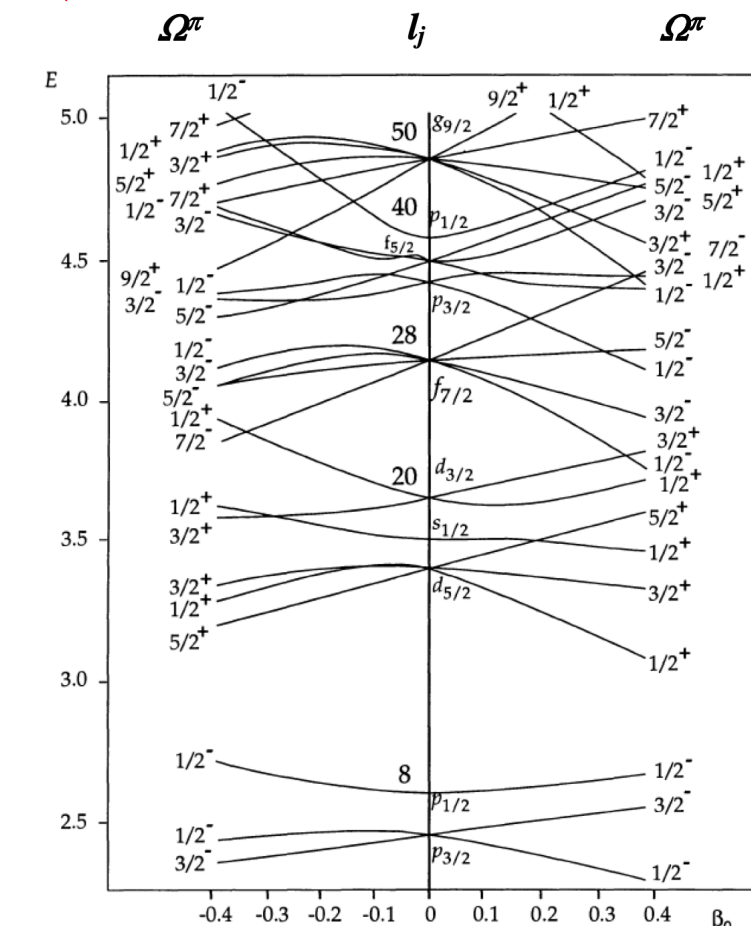
Inclusion of three-body forces

- The normal ordered 2-body approximation breaks rotational symmetry when normal-ordered with respect to a broken symmetry reference state
- Perform spherical HF with fractional filling to normal-order three-nucleon force
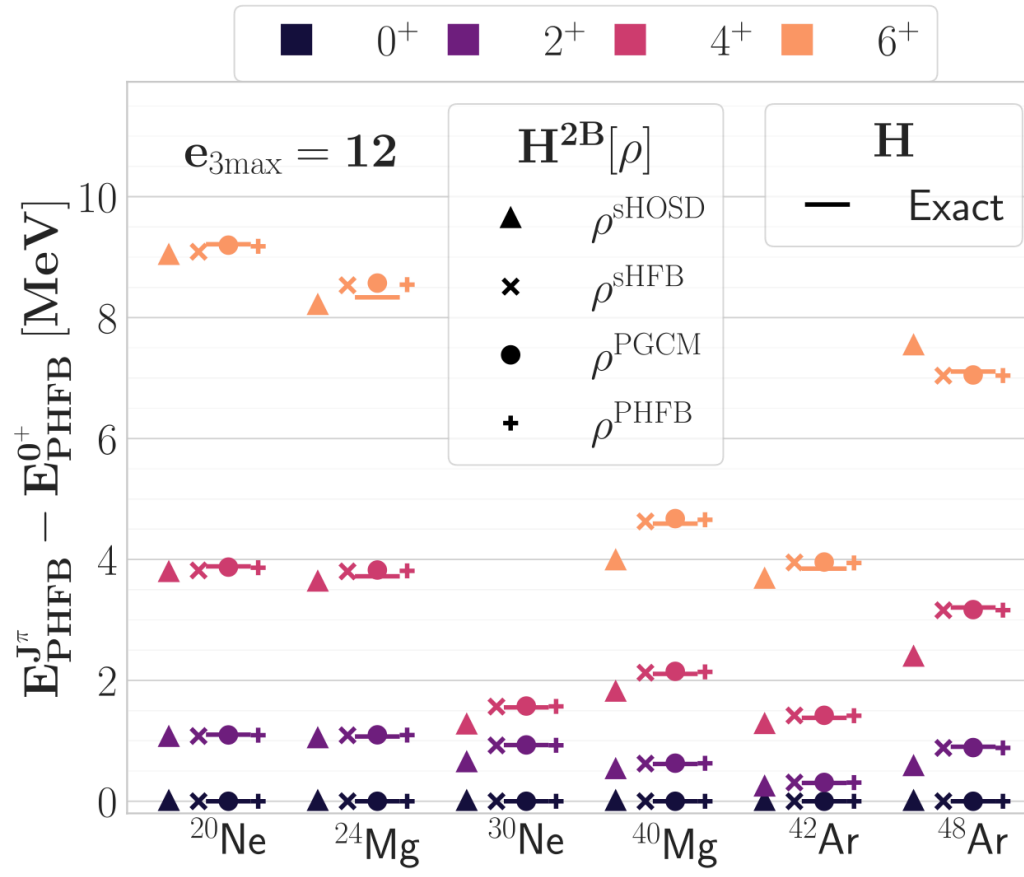
Mikael Frosini et al, Eur. Phys. J. A 57 (2021)
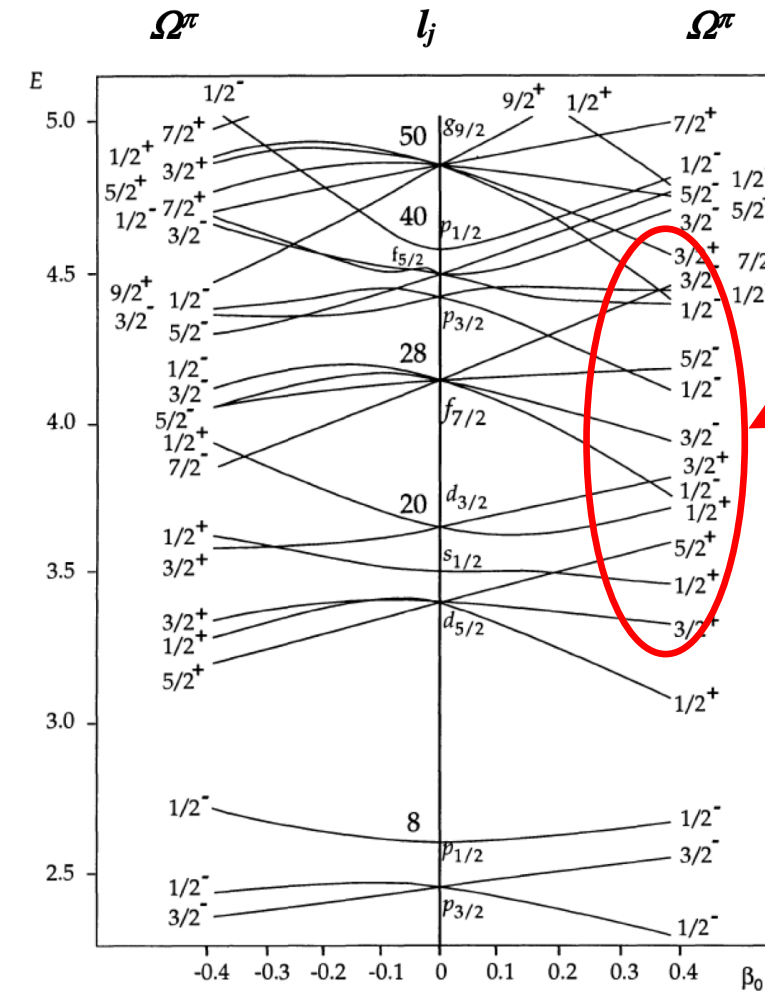
What is the correct spherical filling in very deformed nuclei?

Coupled-cluster computations of deformed nuclei

- Include short-range correlations via coupled-cluster theory
  - Large contribution to total energy
 - Cost increases polynomial with mass

$$|\Psi\rangle = \Omega|\Phi_0\rangle = e^T|\Phi_0\rangle$$

- Include long-range correlations via symmetry projections
  - Small contribution to total energy
  - Relevant for rotational bands and transition matrix elements

$$E^{(J)} = \frac{\langle\widetilde{\Psi}|P_J H|\Psi\rangle}{\langle\widetilde{\Psi}|P_J|\Psi\rangle}$$

S. J. Novario, et al PRC 102, 051303 (2020)


^{20}Ne
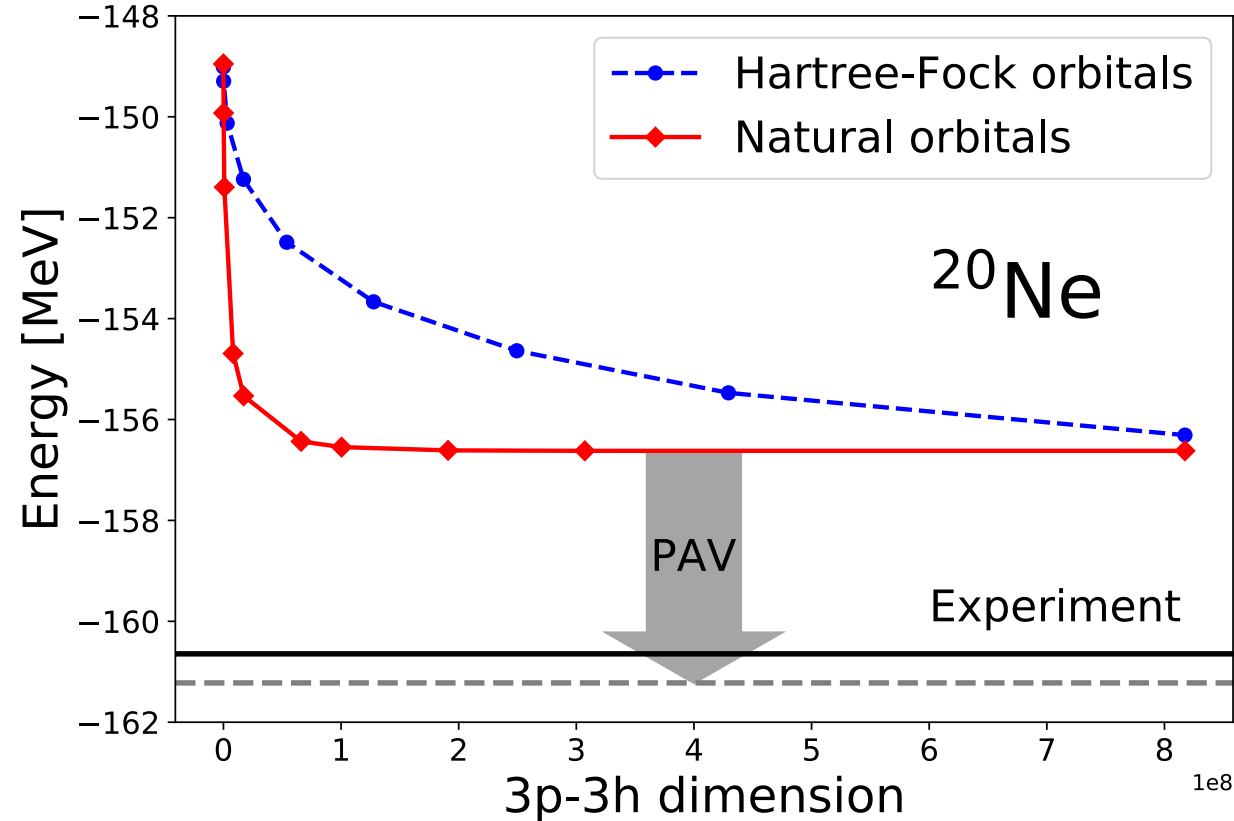
Total energy:

$$E = E_{\text{ref}} + \Delta E_{\text{CC}} + \delta E$$

Neutron-rich nuclei beyond N = 20 are deformed

$$R_{4/2} \equiv \frac{E_{4+}}{E_{2+}}$$

$R_{4/2} = 10/3$ for a rigid rotor

Simple picture: Spherical states (magic $N = 20$ number in the traditional shell model) coexist with deformed ground states

Poves & Retamosa (1987); Warburton, Becker, and Brown (1990); …
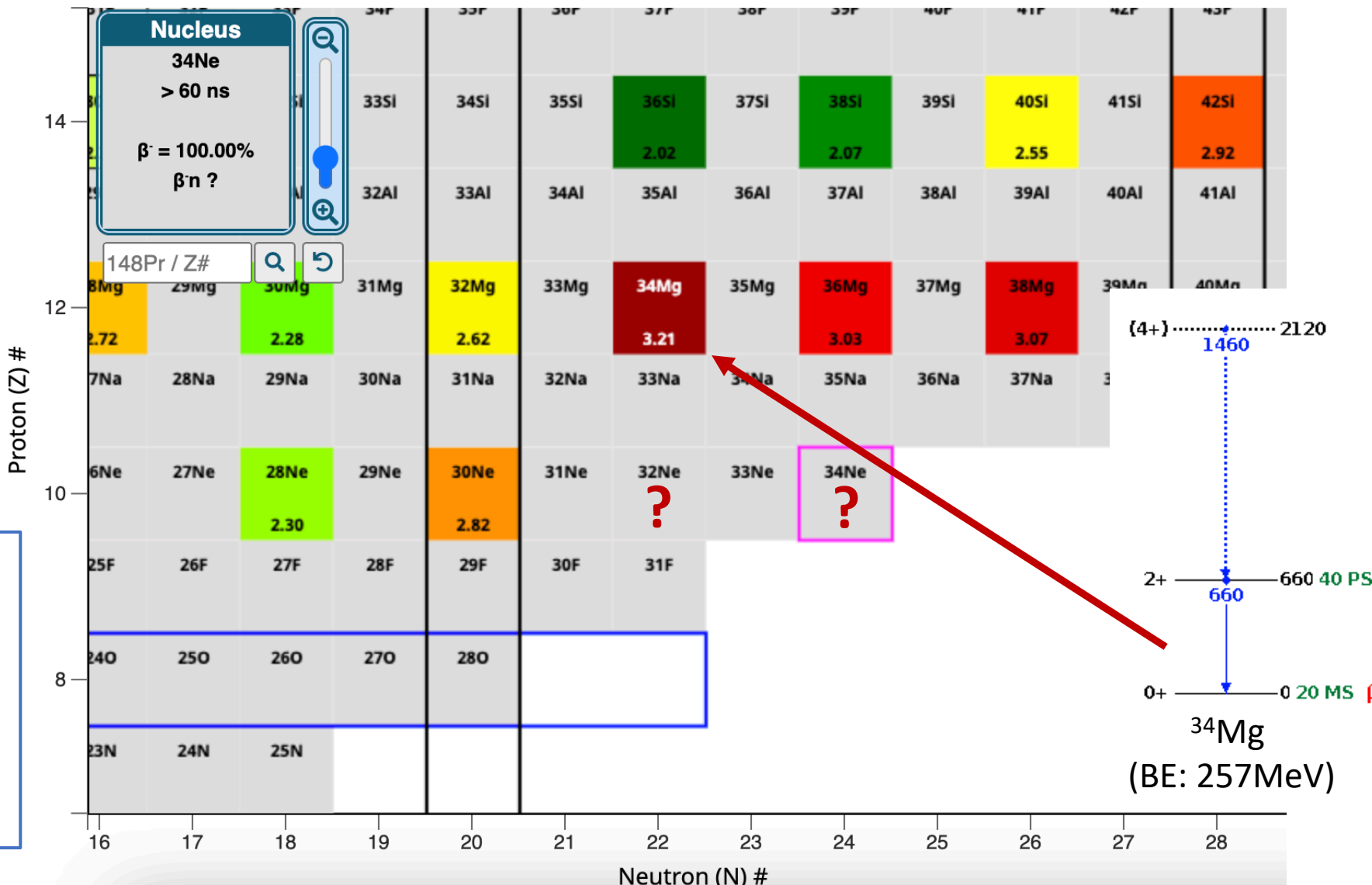
Collectivity in neon isotopes
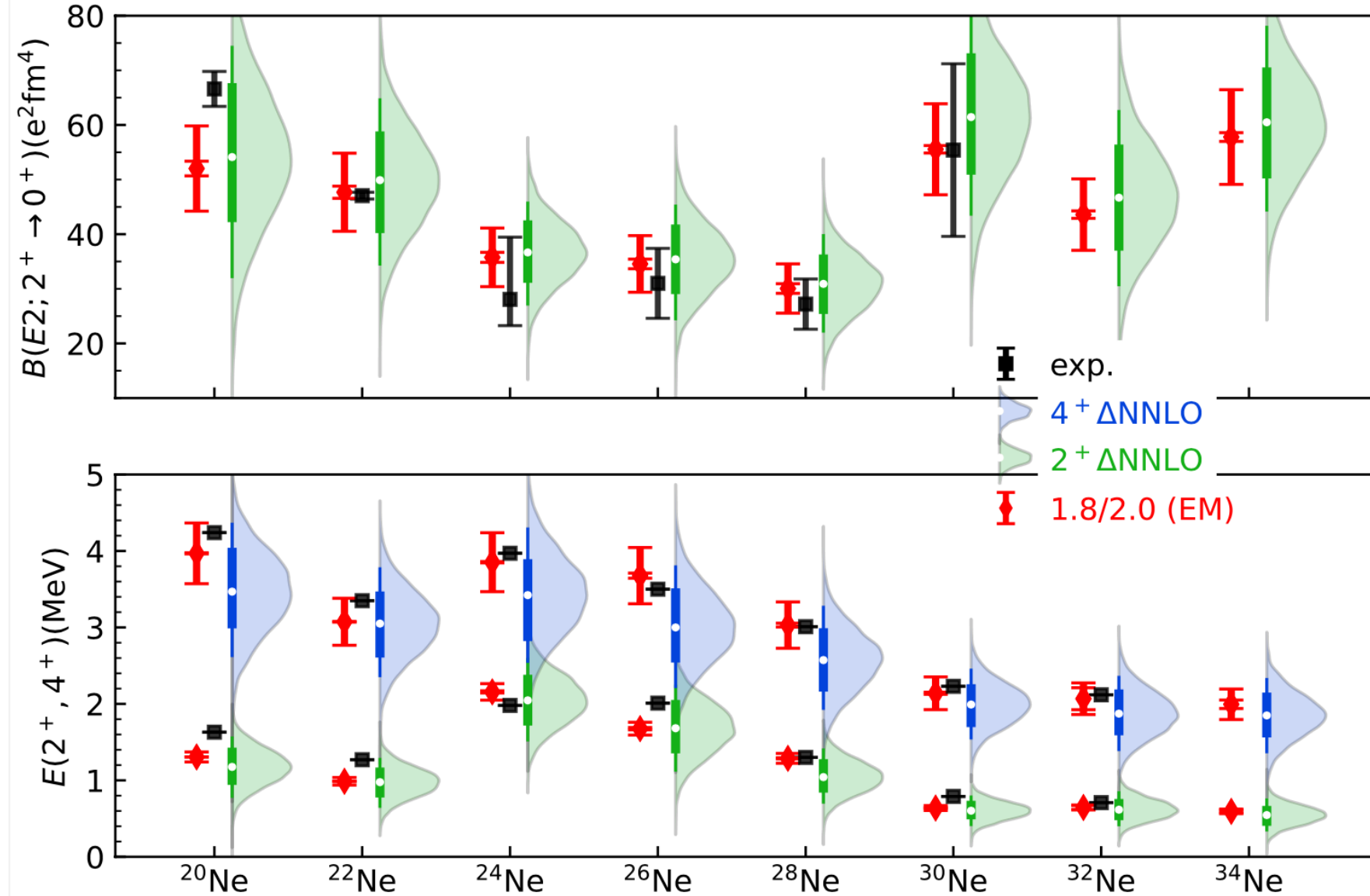
- Calculations follow data
- No effective charges
- Spectra of $^{30-34}$Ne follow that of a rigid rotor
- Small energies reflect a large moment of inertia and a strong deformation

Ensemble of delta-full interactions from recent study of ^{28}O

Y. Kondo et al.,
Nature **620**, 965–970 (2023)

Zhonghao Sun, A. Ekstrom, C. Forssen, G. Hagen. G. R. Jansen, T. Papenbrock arXiv:2404.00058 (2024)

Shape co-existence in ^{30}Ne
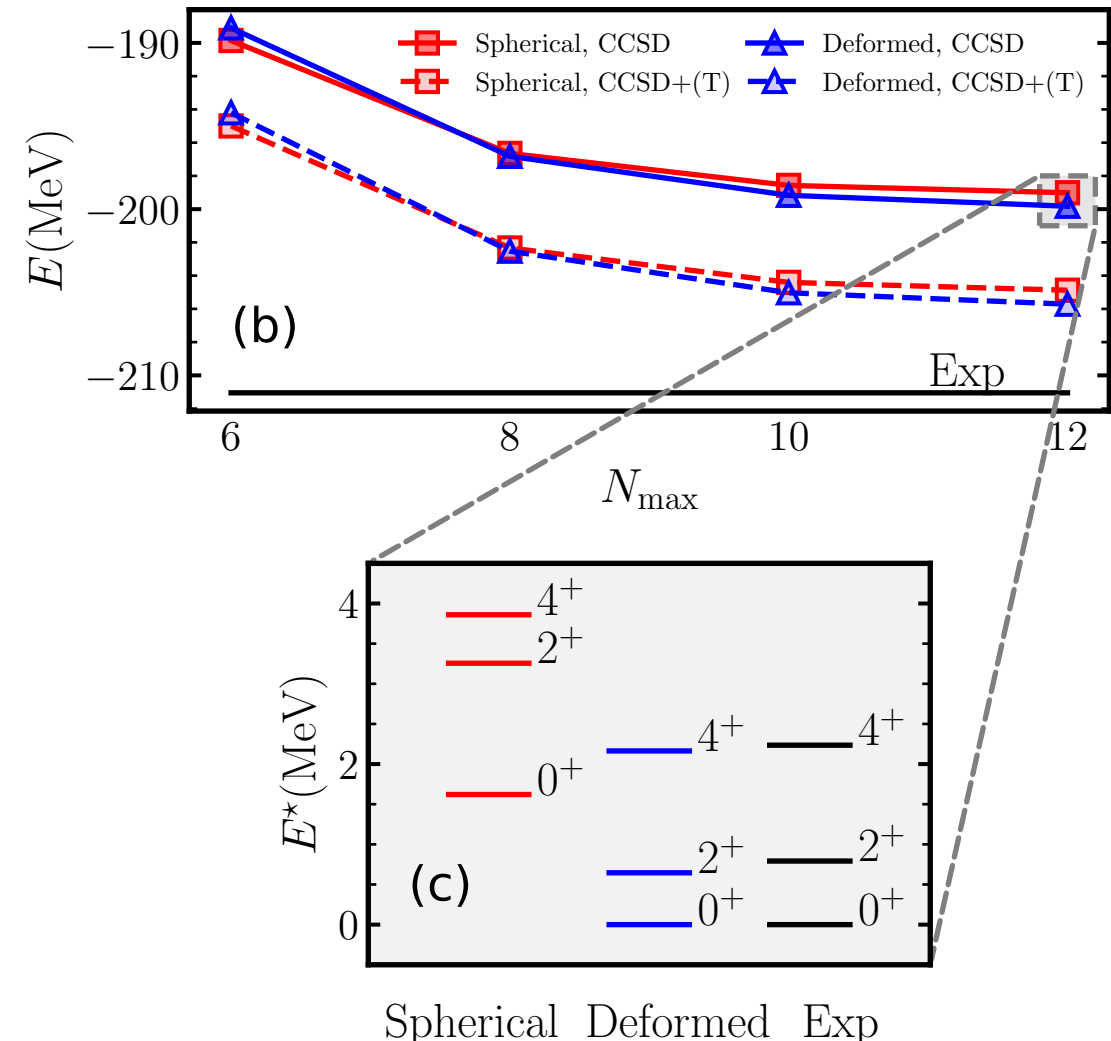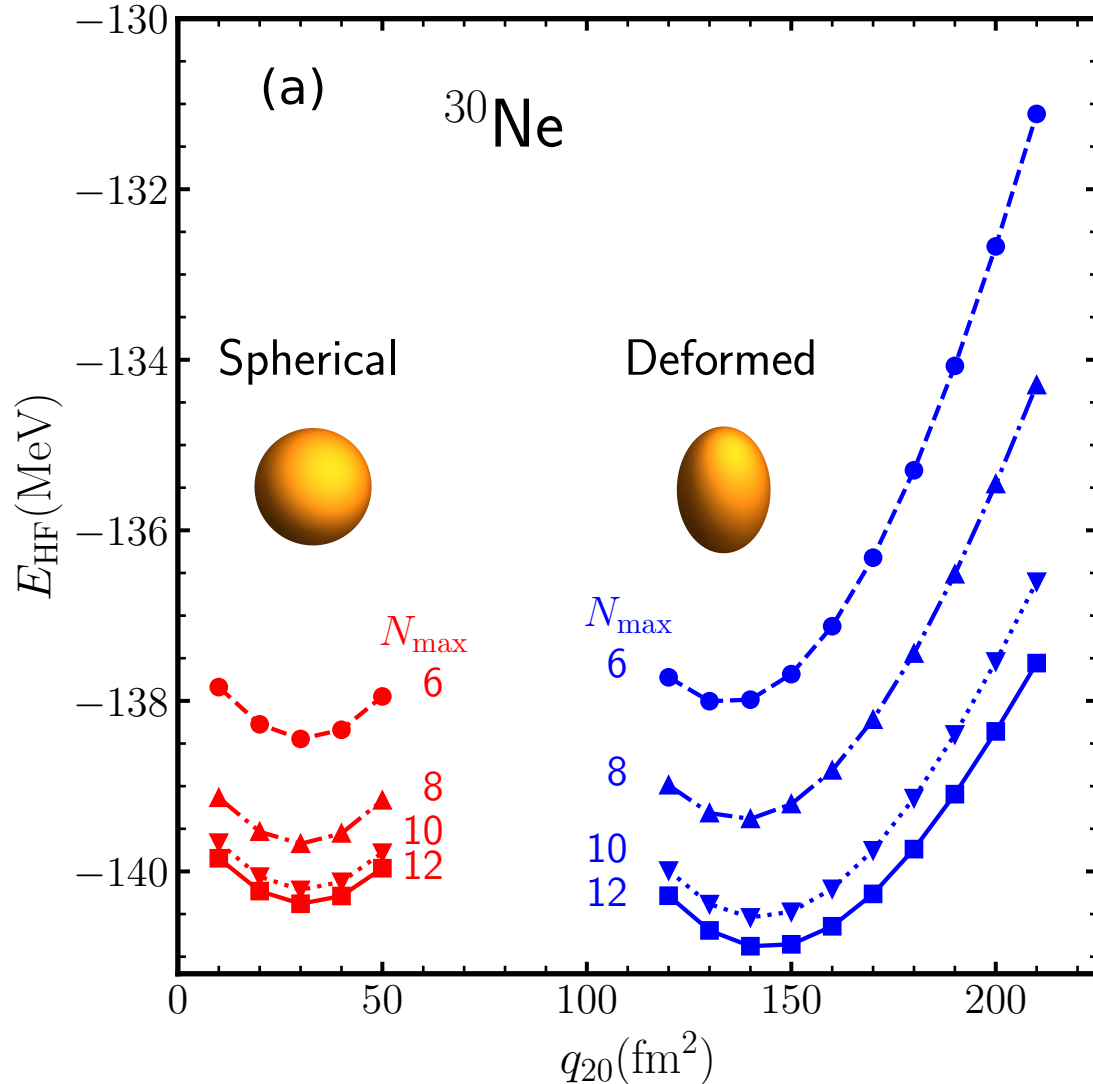
Making sense of spectra in odd-mass nuclei

Looks complicated;
shown data lacks understanding

$^{9}_{4}Be_{5}$
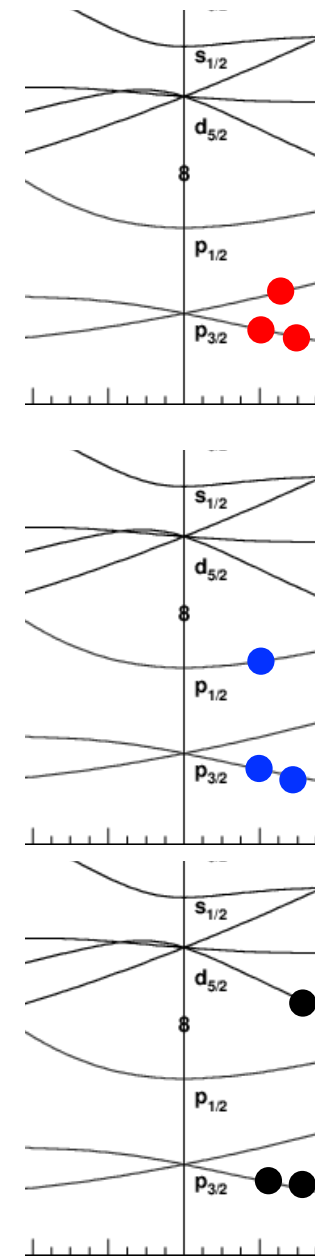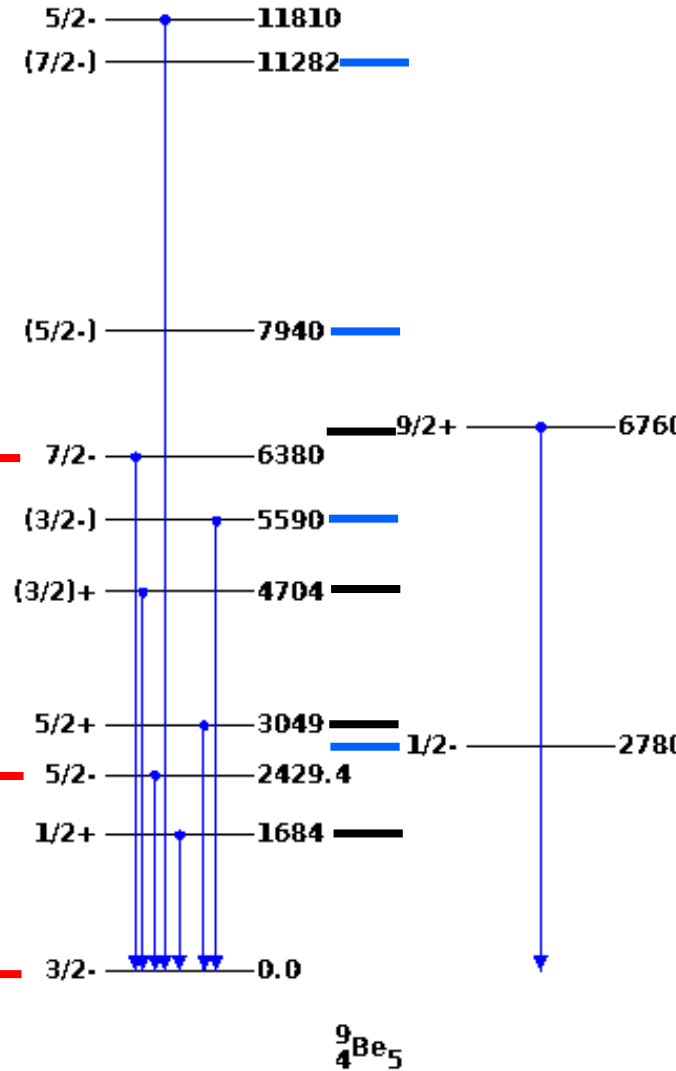
Zhonghao Sun et al., arXiv:2409.02279 (2024)
Hartree-Fock computations yield deformed reference
Coupled-cluster + projection yields bands
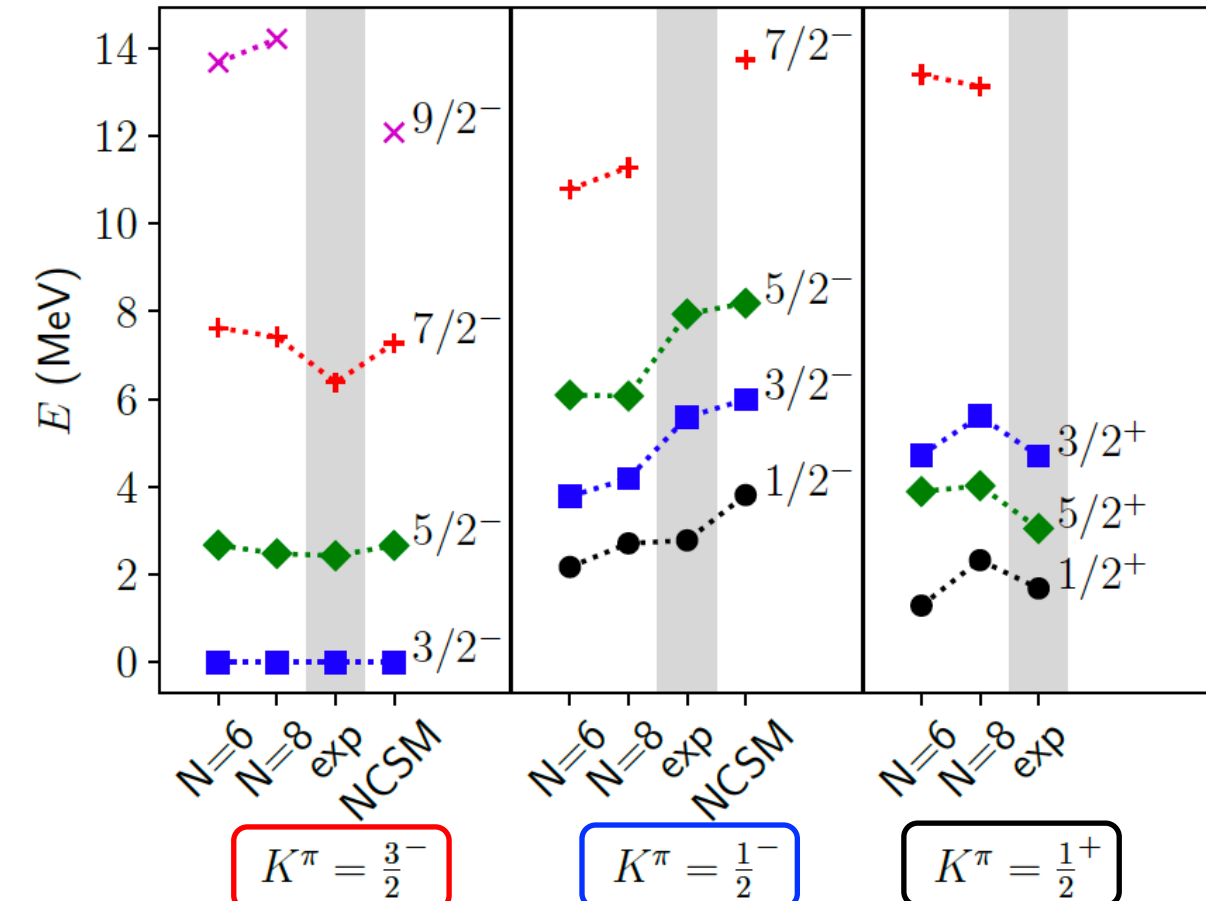
NCSM from Caprio, Maris, Vary & Smith,
Int. J. Mod. Phys. E 24, 1541002 (2015)

Rotational bands in odd-mass magnesium

Zhonghao Sun et al., arXiv:2409.02279 (2024)
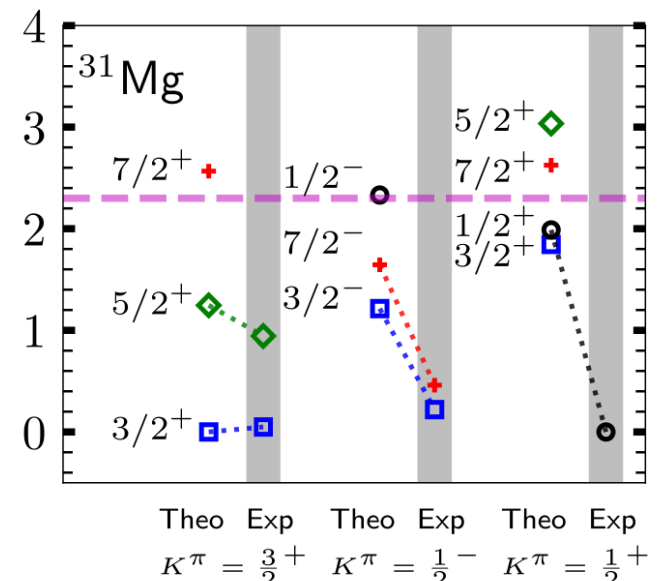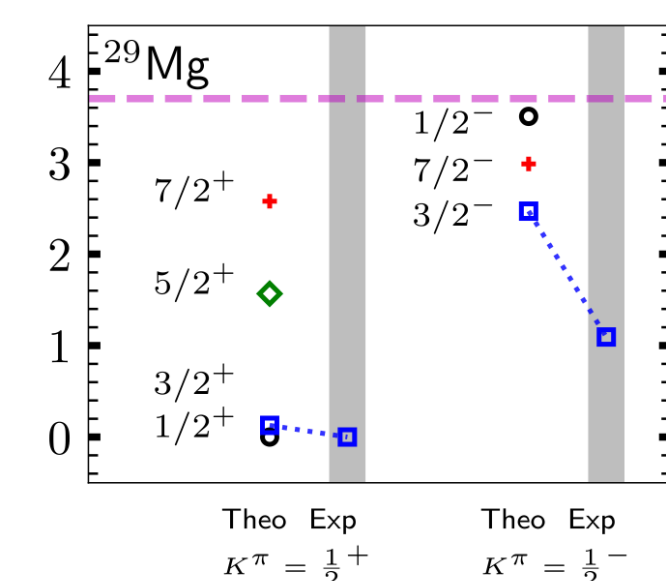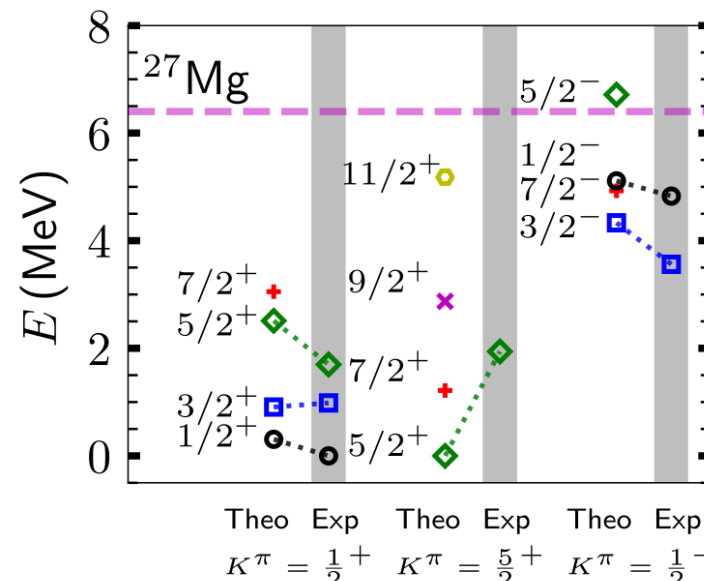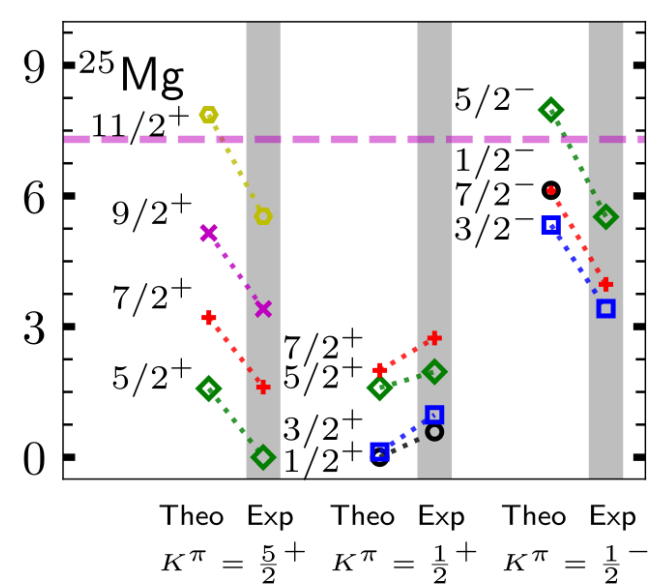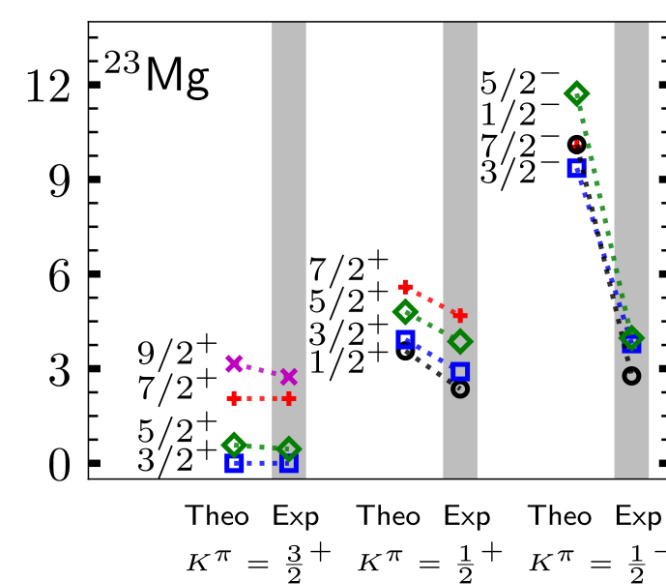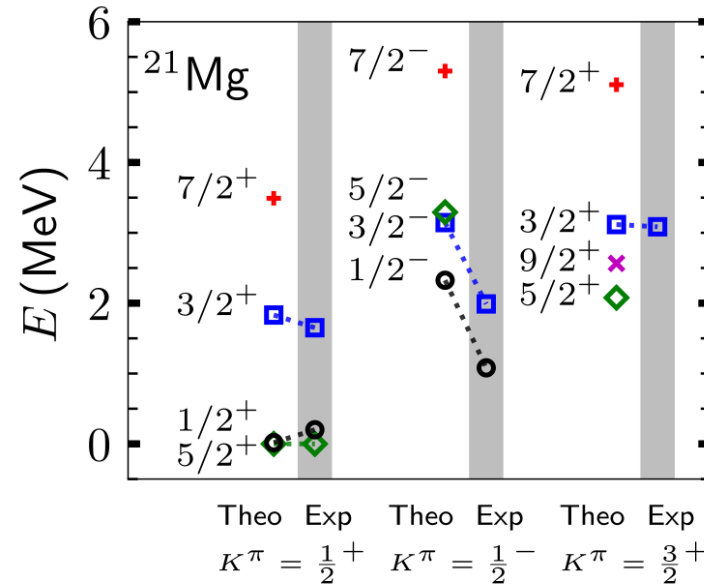
Strongly deformed nuclei around ^{80}Zr

Tomás R. Rodríguez, J. Luis Egido,
Phys. Lett. B 705 255 (2011)
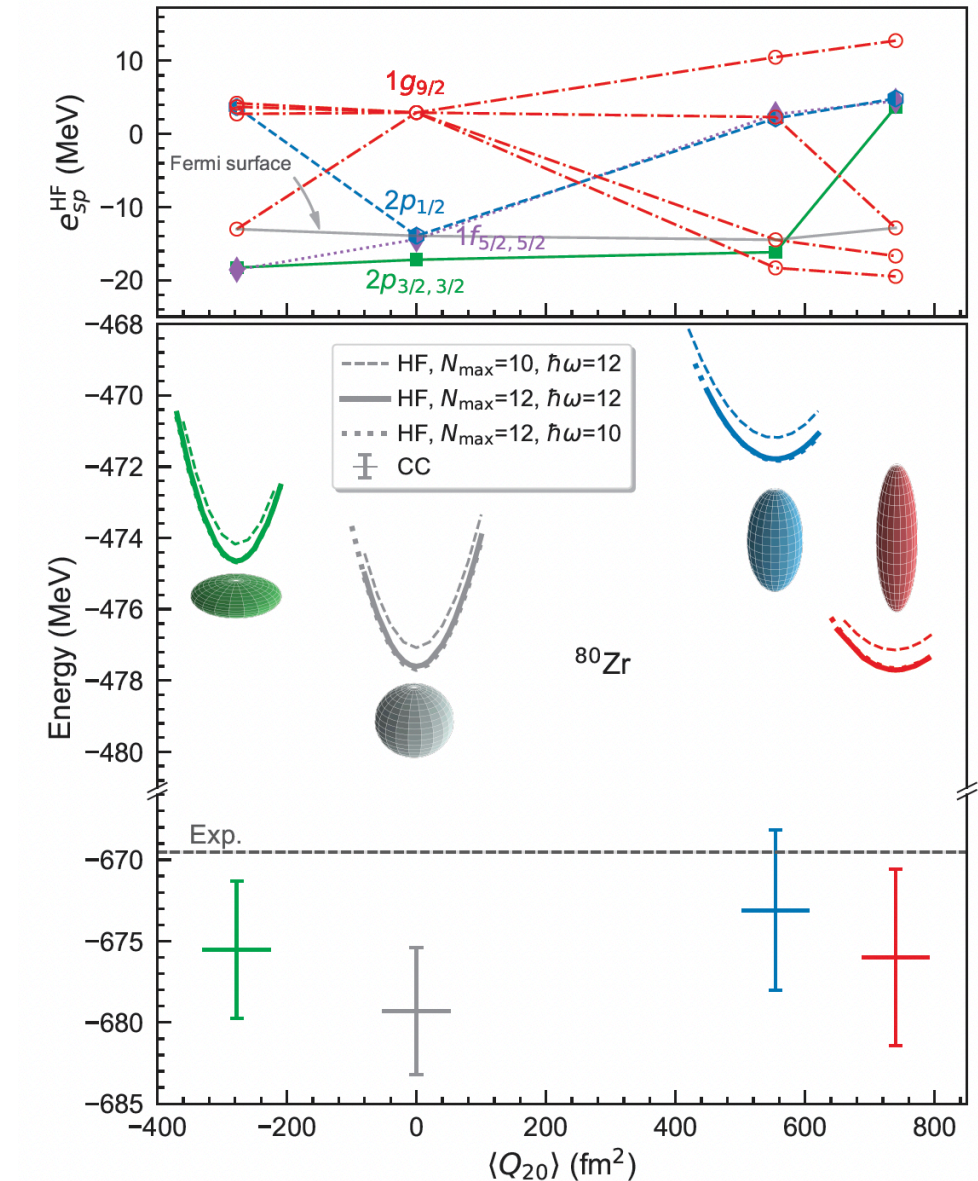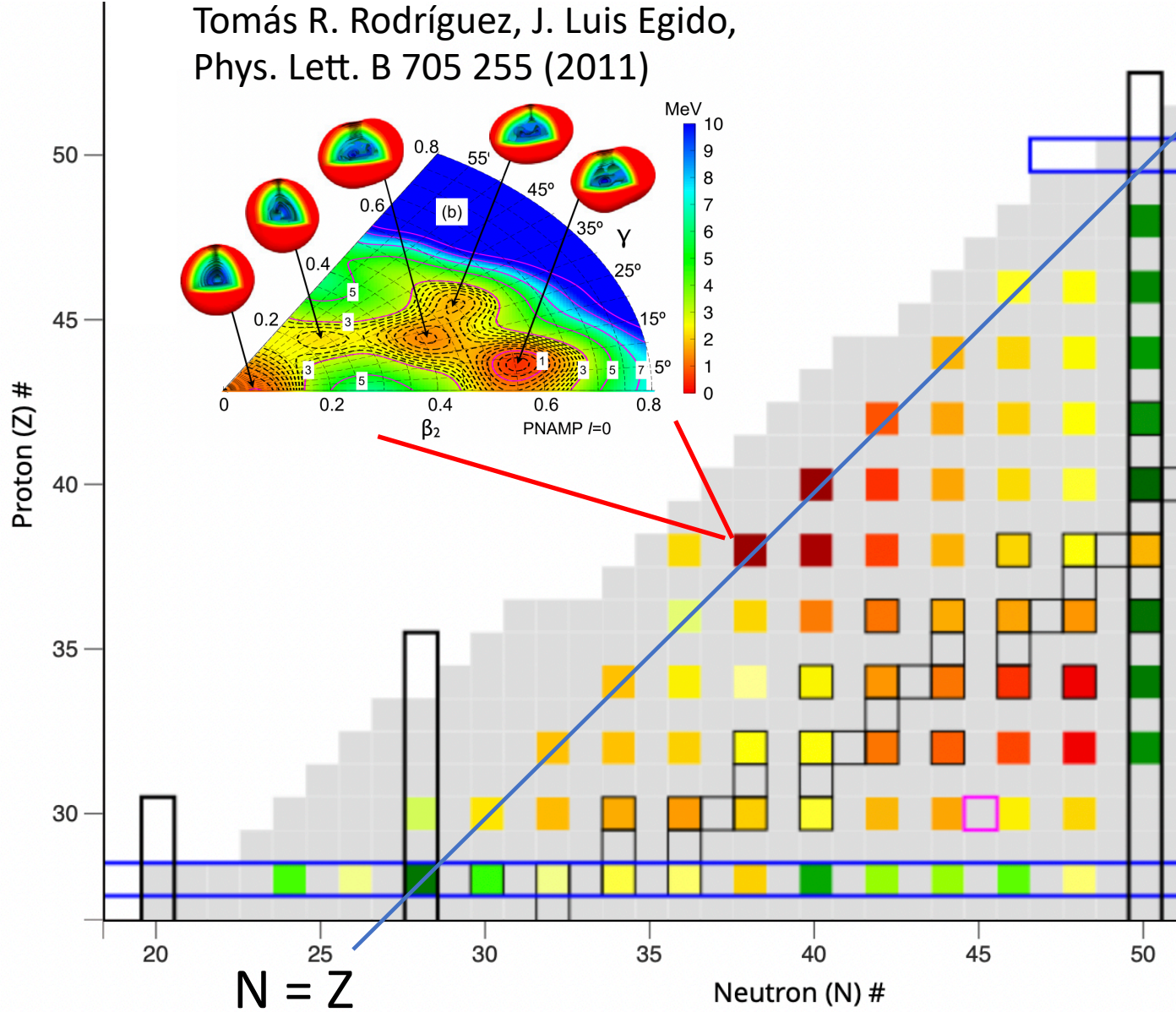
^{80}Zr

Baishan Hu, Zhonghao Sun, G. Hagen, T. Papenbrock.
Phys. Rev. C **110**, L011302 (2024)

Coupled-cluster computations of strongly deformed nuclei around ^{80}Zr

Spectrum prefers larger prolate shape
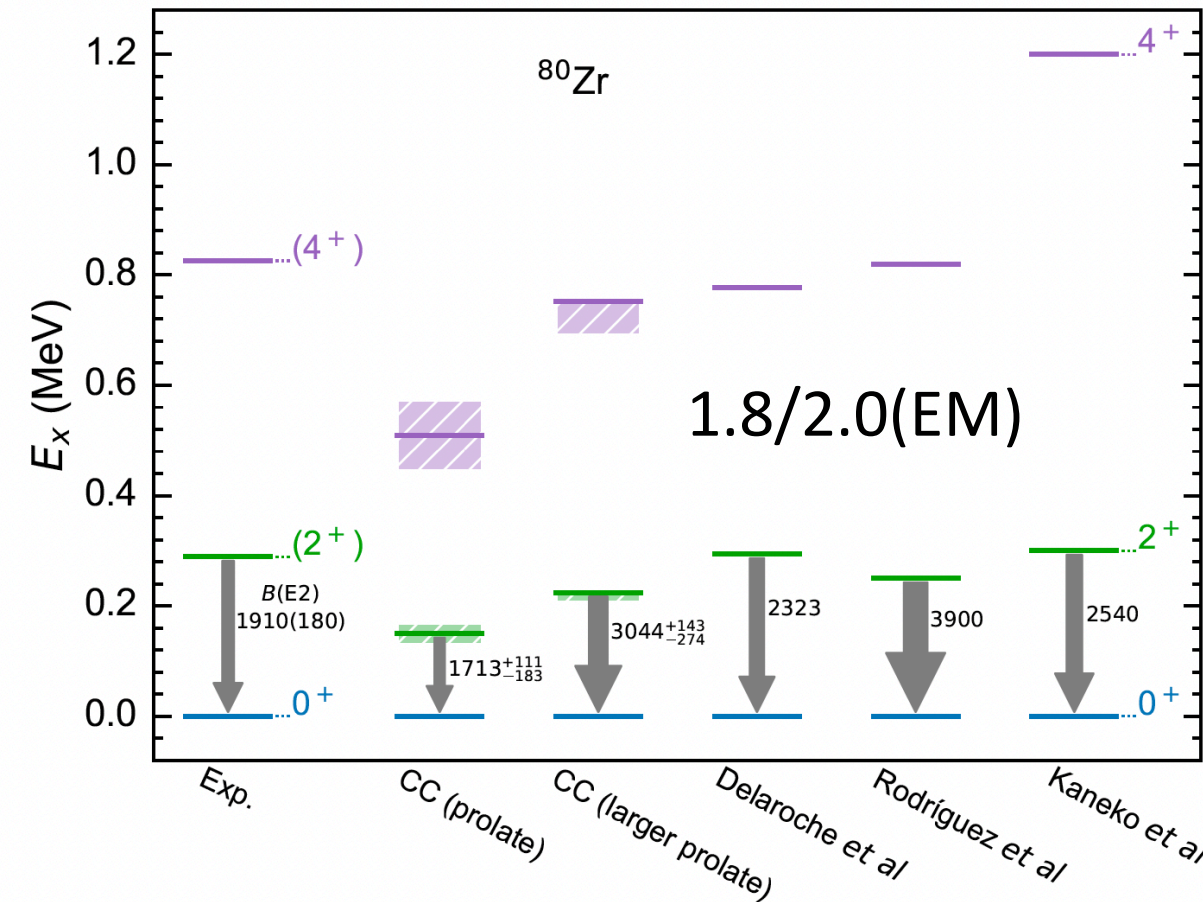
$B(E2)$ prefers prolate band

Deformation "south" of ^{78}Ni

^{68}Ni

oblate deformation

prolate deformation

spherical

R. Taniuchi, et al, Nature **569**, 53 (2019)

^{4}He ^{16}O ^{40}Ca ^{48}Ca ^{56}Ni ^{78}Ni (this work) ^{132}Sn ^{208}Pb

^{68}Ni

$E(2_1^+)$ (MeV)

Protons, Z

Neutrons, N

Two-neutron drip line
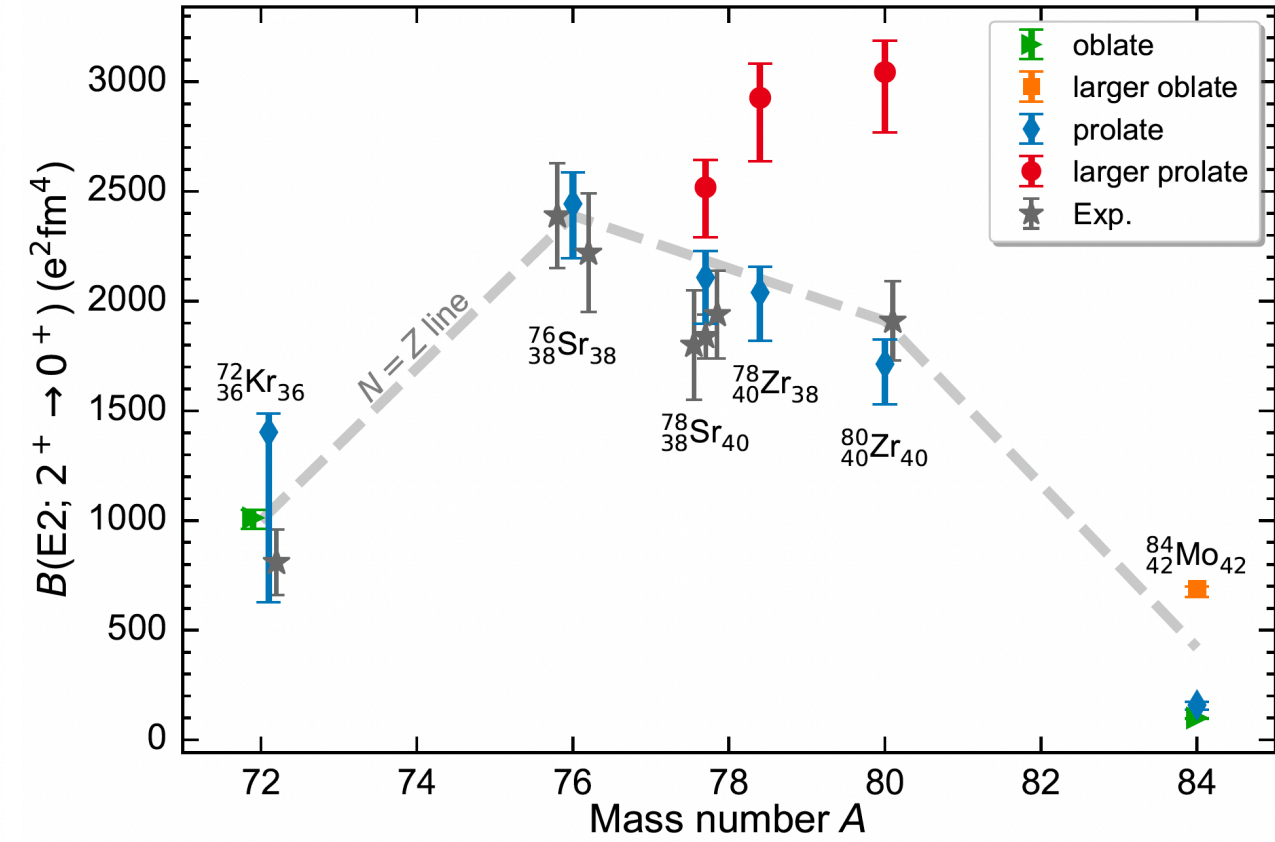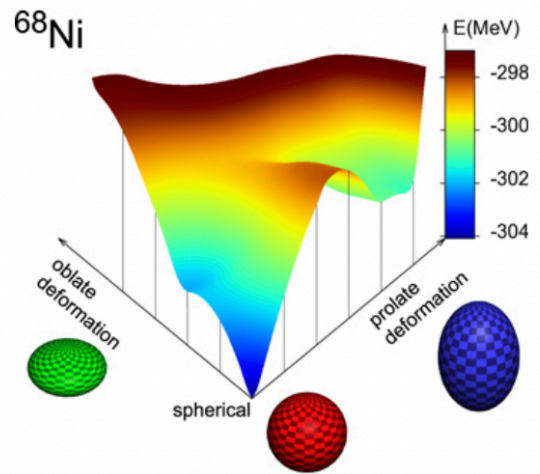
T Otsuka and Y Tsunoda *J. Phys. G* **43** 024009 (2016)

Neutron (N) #
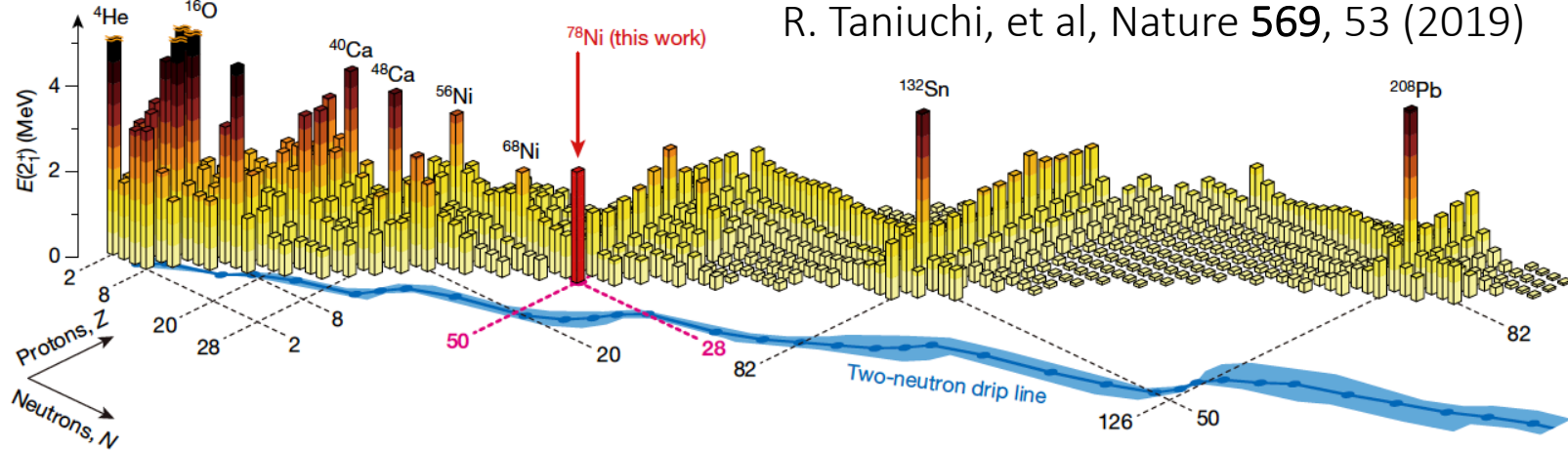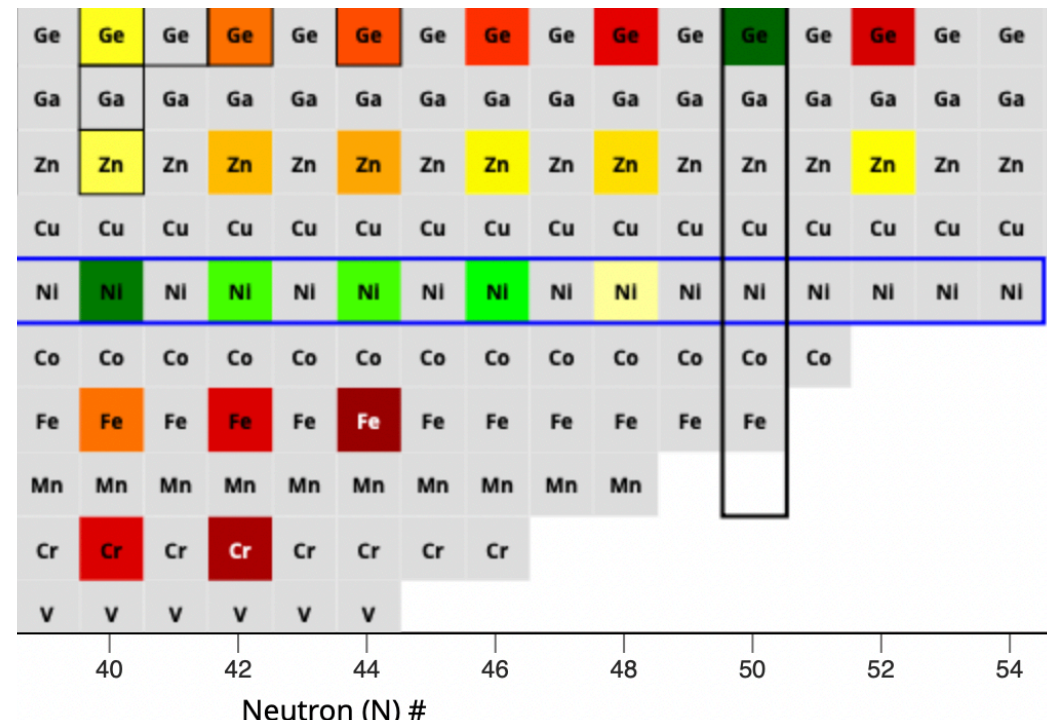
Deformed band?
Where is the band head?
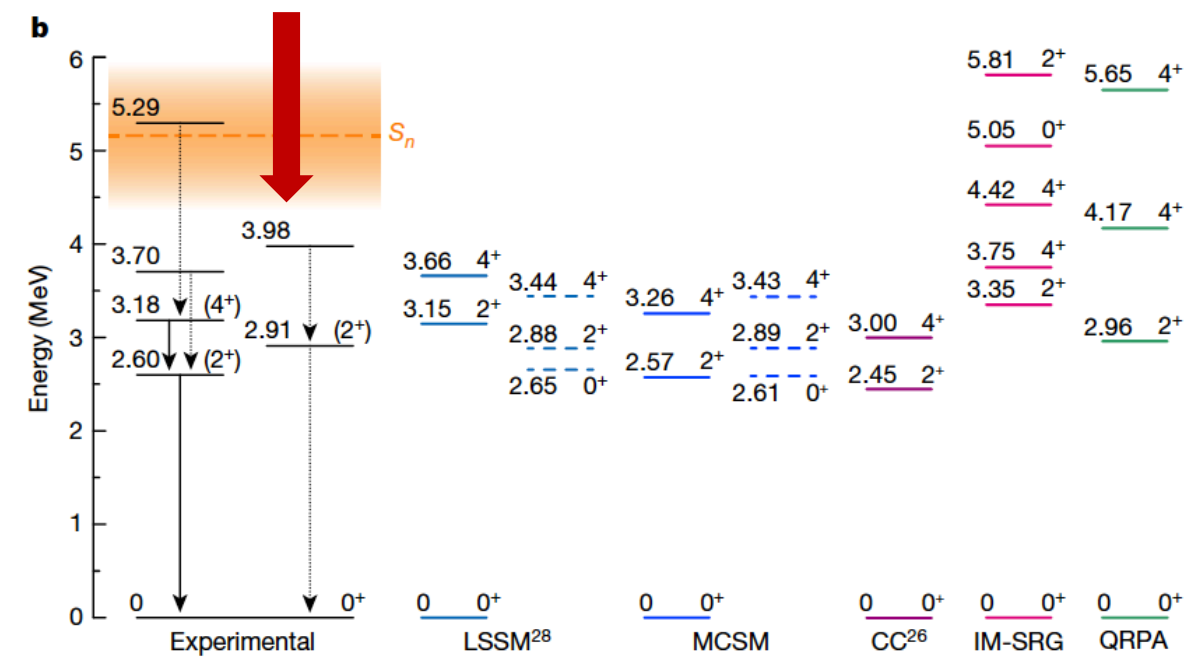
Deformation "south" of ^{78}Ni

- Erosion of the magic number N = 50 toward ^{70}Ca manifested by onset of deformation in the ground-states
- For ^{78}Ni we predict a low-lying rotational band consistent with recent data and other

B. Hu et al Phys. Lett. B **858**, 139010 (2024)
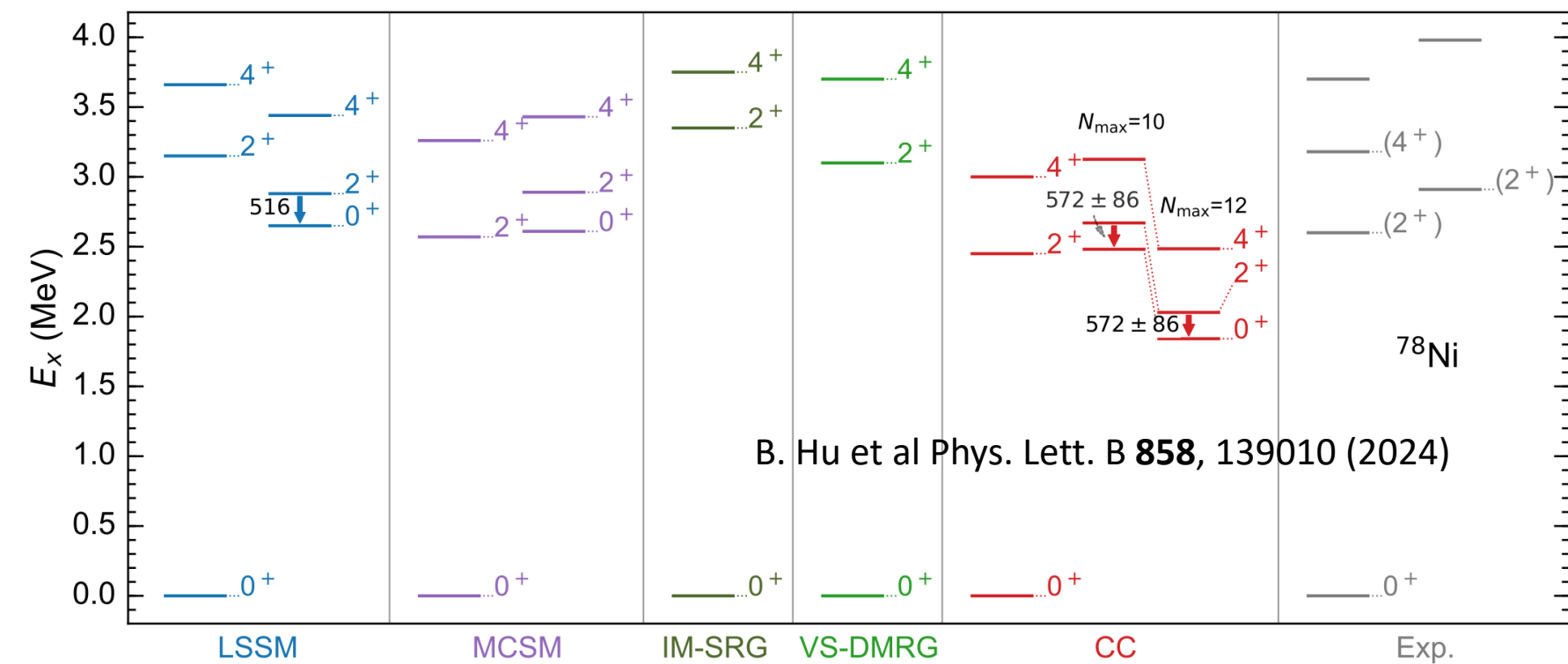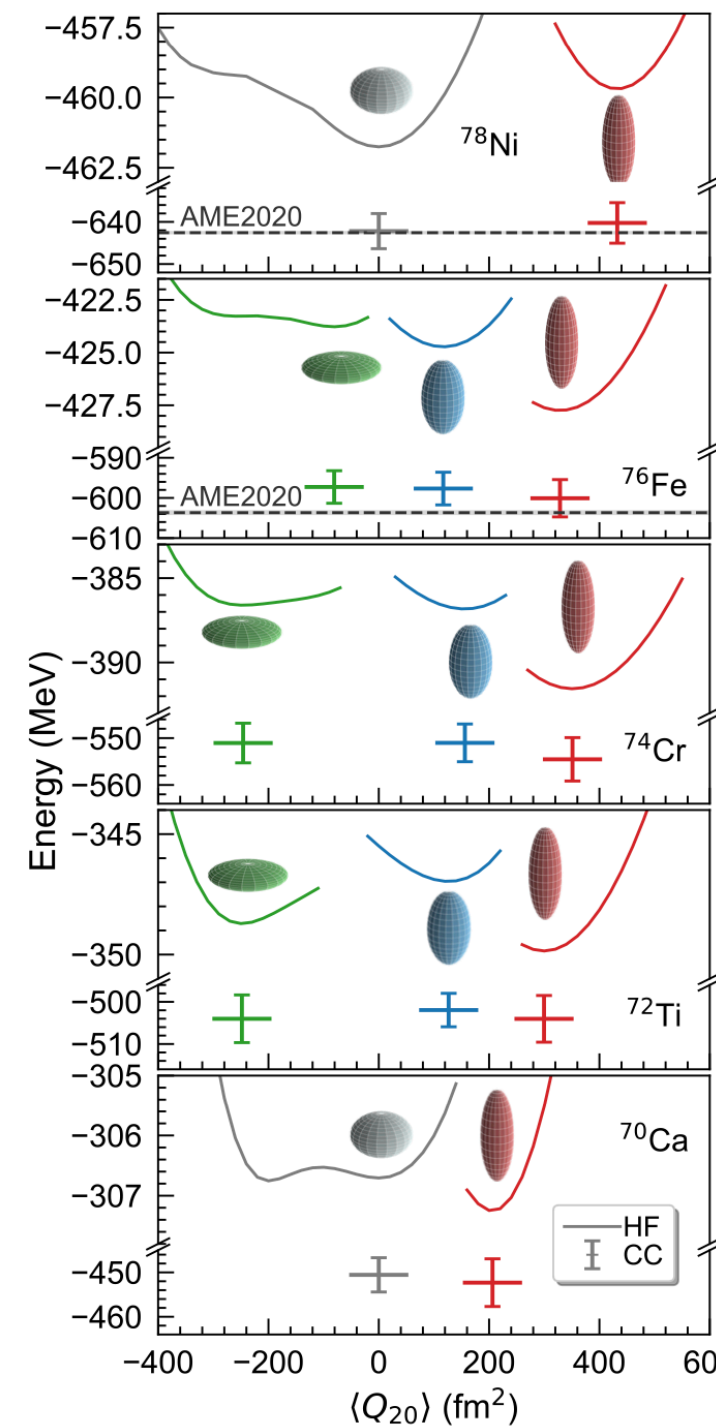
VS-DMRG: A. Tichai, et al, PLB 855, 138841 (2024)
MCSM: R. Taniuchi, et al, Nature 569, 53 (2019)
LSSM: F. Nowacki, et al, PRL 117, 272501 (2016)

Deformation "south" of ^{78}Ni

spectra largely agree with shell-model results within our uncertainty estimates
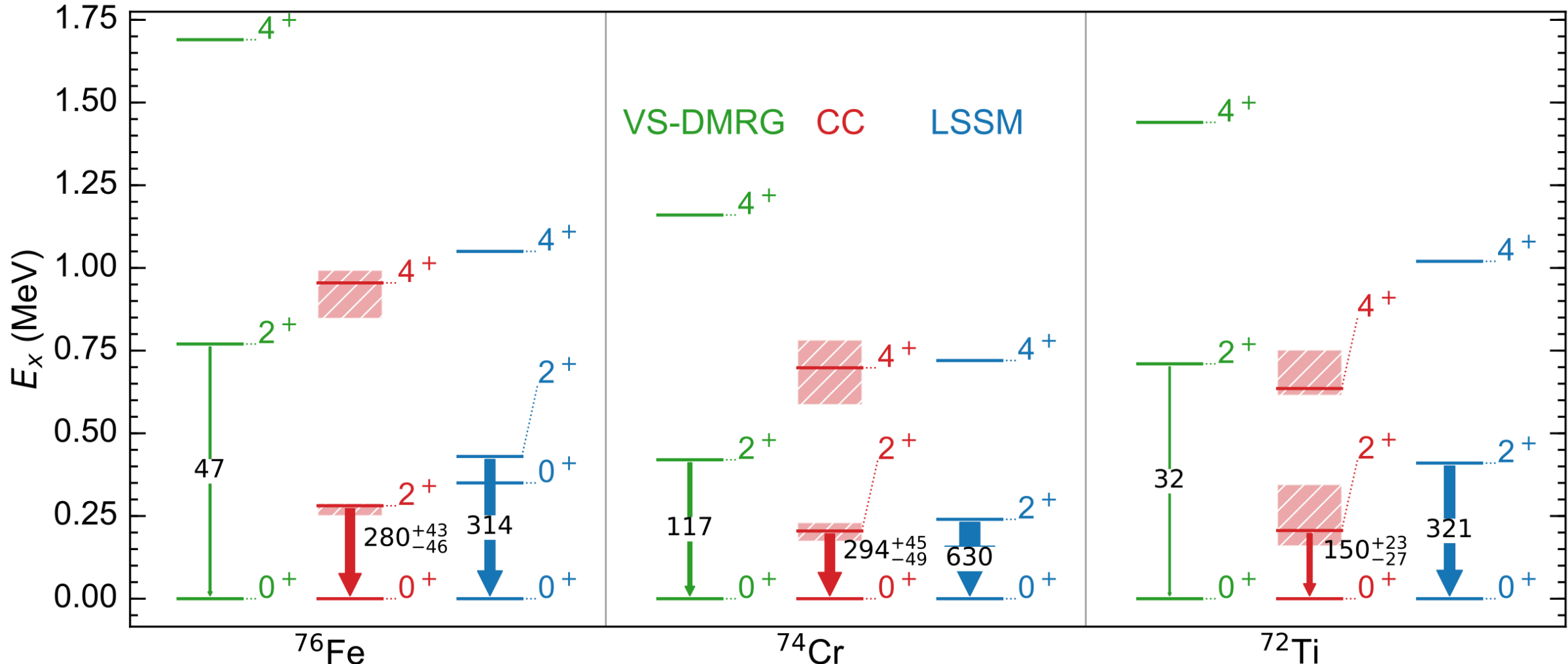
What drives deformation in nuclei?

- 50's: surface vibrations of a liquid drop (Bohr/Mottelson)
- 60's: competition between pairing and quadrupole interactions from HFB calculations in two shells (Baranger/Kumar)
- 70's: isoscalar neutron-proton interactions dominate over isovector pairing from shell model (Federman/Pittel, Dufour/Zuker)
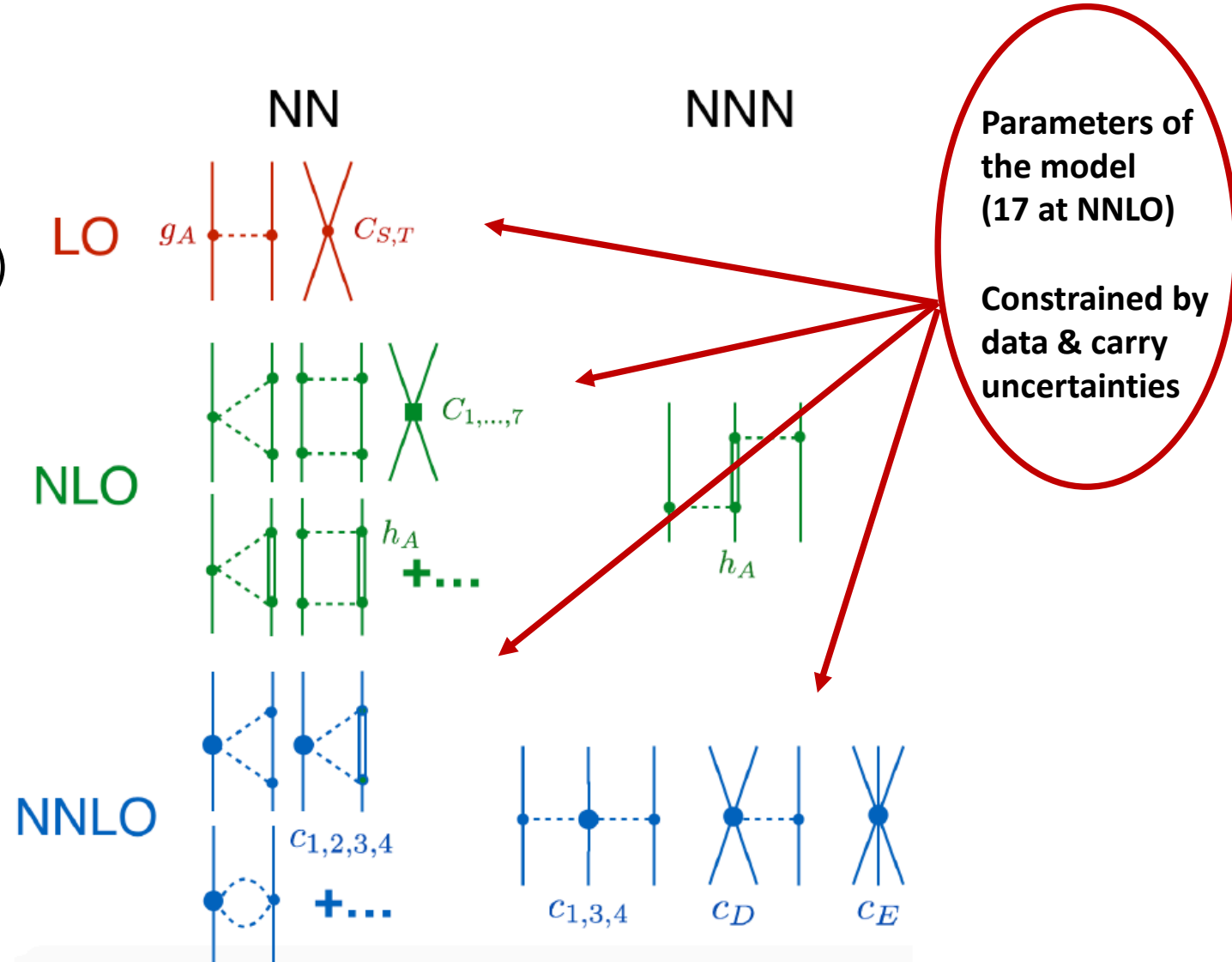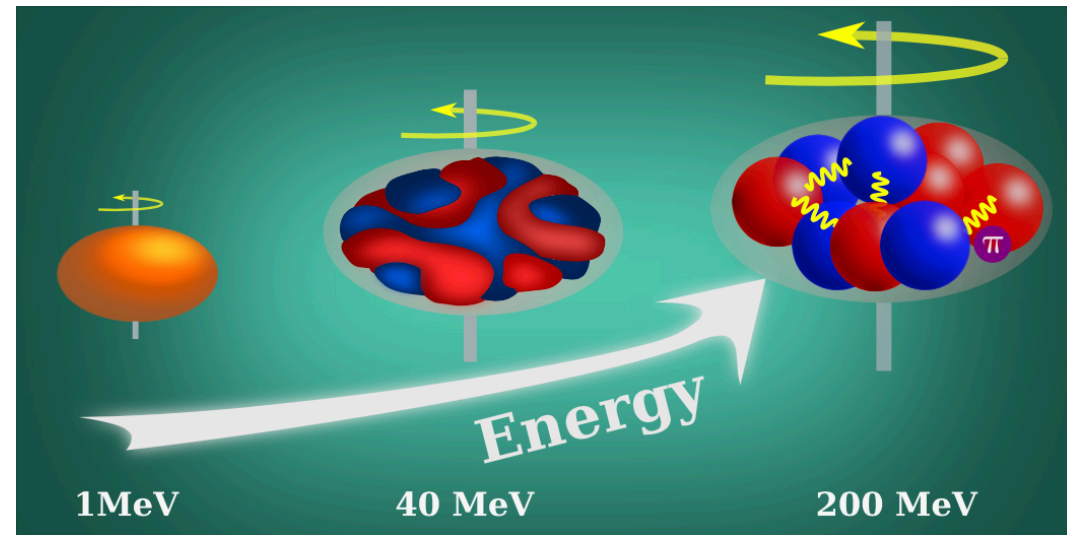
Nuclear deformation viewed at different resolution scales

NN   NNN

LO g_A $C_{S,T}$

NLO $C_{1,\dots,7}$ h_A +... h_A

NNLO $c_{1,2,3,4}$ +... $c_{1,3,4}$ c_D c_E

Parameters of the model (17 at NNLO)

Constrained by data & carry uncertainties

Global sensitivity analysis

Sensitivity analysis addresses the question 'How much does each model parameter contribute to the uncertainty in the prediction?'

Global methods deal with the uncertainties of the outputs due to input variations over the whole domain.

Computational bottleneck

A global sensitivity analyses of properties of atomic nuclei typically would require more than one million model evaluations

Sensitivity analysis of the radius and binding energy of ^{16}O

Andreas Ekström, Gaute Hagen PRL **123**, 252501 (2019)

Reduced order model for deformed states

Parameter domain

$\vec{\alpha}_2$ $\vec{\alpha}_1$

$\vec{\alpha}_\odot$

$\vec{\alpha}_4$

$\vec{\alpha}_3$

Latin Hypercube Sampling
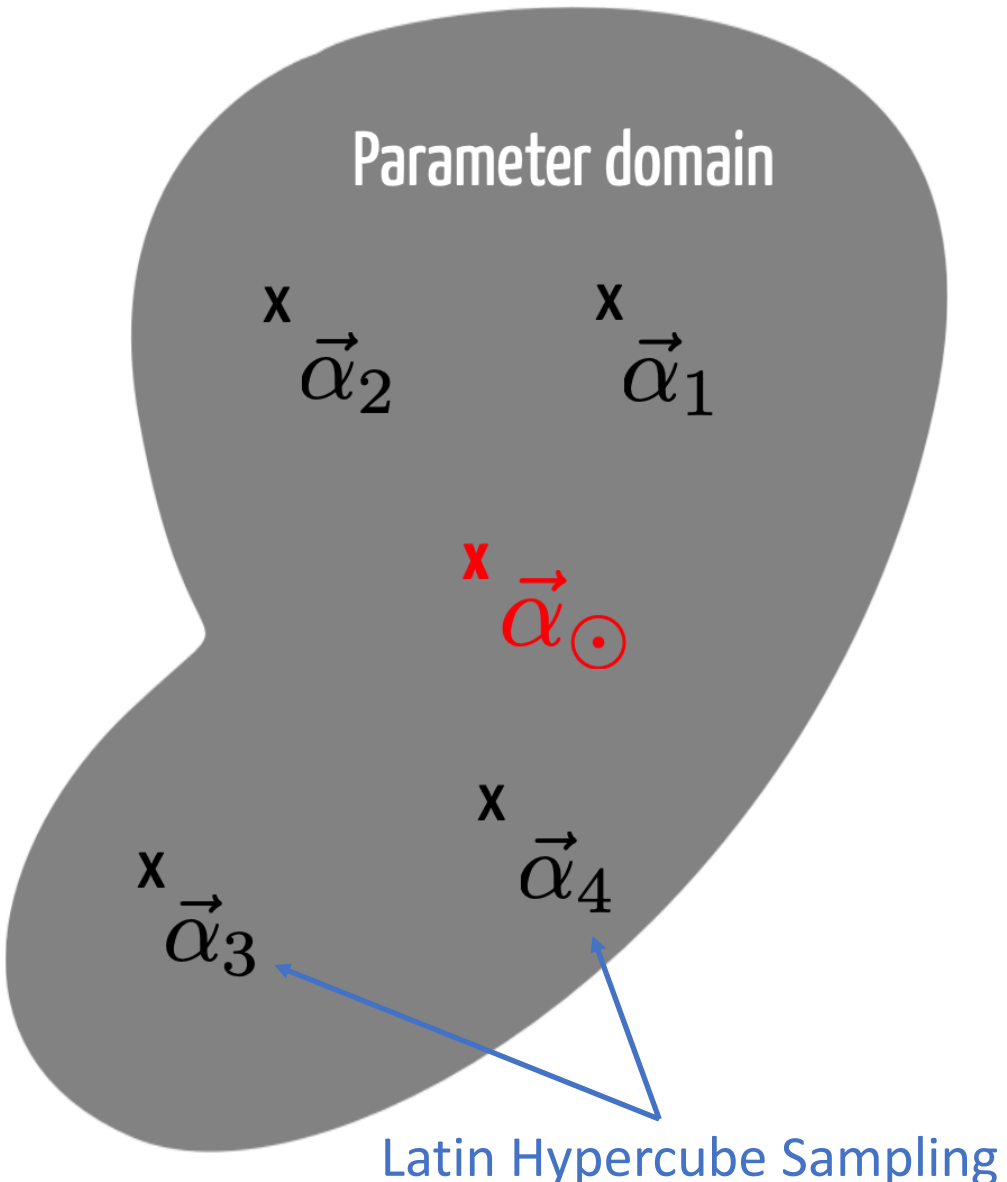
- Eigenvector continuation method [Frame D. et al., Phys. Rev. Lett. 121, 032501 (2018), A. Ekström, G. Hagen PRL 123, 252501 (2019), S. König et al Phys. Lett. B 810 (2020) 135814]

- Write the Hamiltonian in a linearized form

$$H(\vec{\alpha}) = h_0 + \sum_{i=1}^{N_{\mathrm{LECs}}=17} \alpha_i h_i$$

- Select "training points" (snap-shots) where we solve the exact problem

- Project a target Hamiltonian onto sub-space of training vectors and diagonalize the generalized eigenvalue problem

$$\mathbf{H}(\vec{\alpha}_\odot)\, \vec{c} = E(\vec{\alpha}_\odot)\, \mathbf{N}\, \vec{c},$$

Computing nuclei at lightning speed

(~5 mins: ~10^5 energy/radius calculations of ^{16}O)
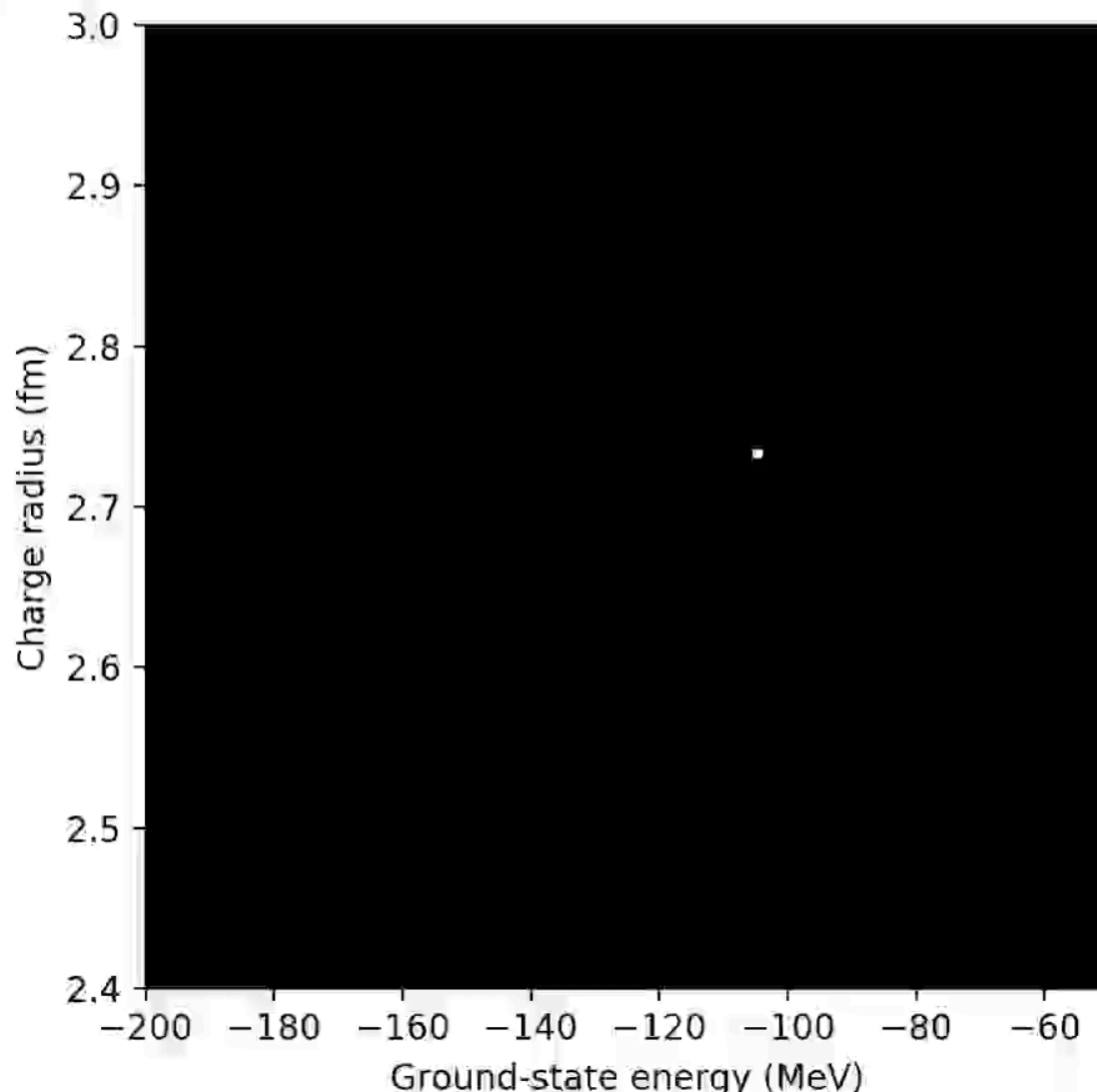
Realtime speed and accuracy of emulated ground-state energy and charge radius of ^{16}O for different values of interaction parameters

$$H(\vec{\alpha}) = \sum_{i=0}^{N_{\text{LECs}}=16} \alpha_i h_i$$

Accuracy: roughly the pixel size

Speedup: 20 years of single node computations can be replaced by a 1 hour run on a laptop

Andreas Ekström, Gaute Hagen PRL **123**, 252501 (2019)

Linking deformation to nuclear forces
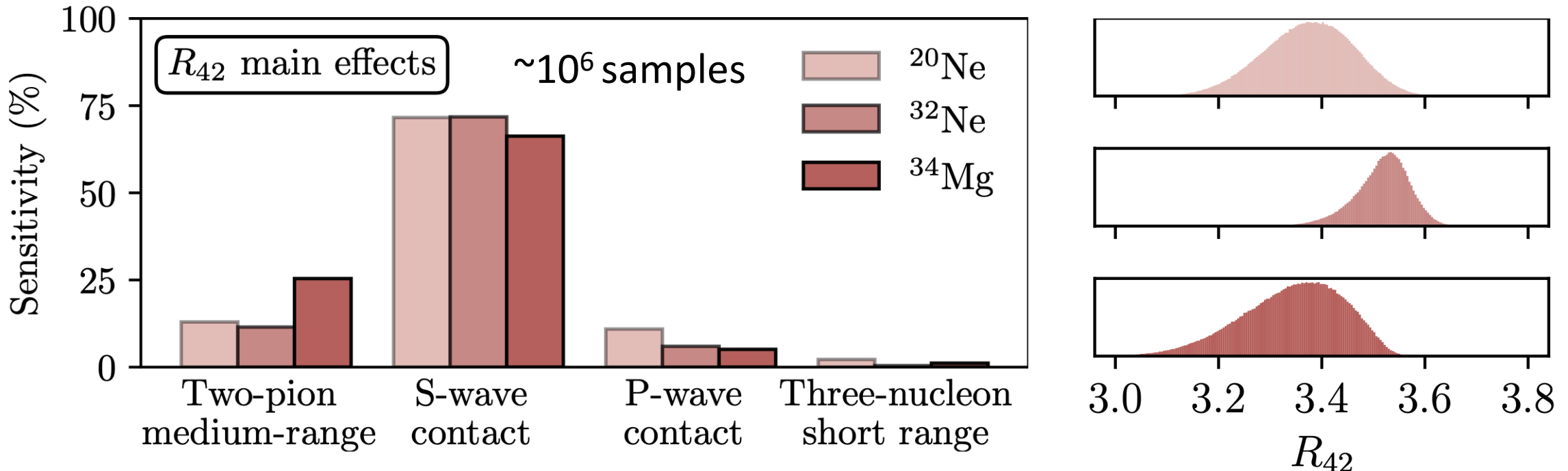
- More than 50% of the deformation is driven by the S-wave contact part of the interaction
- Adding short-range repulsion increase deformation presumably by reducing pairing
- Medium-range two-pion exchange is also important. Increasing its strength increases deformation, presumably by adding attraction in higher partial waves

Summary

Breaking and restoring symmetries

Exploits separation of scale between collective and specific UV physics

Conceptually simple & computationally affordable

- Shape coexistence in ^{30}Ne and ^{32}Mg

- Rotational bands in odd mass neon and magnesium isotopes

- Much improved B(E2) values with no effective charges in ^{3x}Ne, ^{3x}Mg, ^{80}Zr

- Connected deformation to microscopic forces

- Predict low-lying rotational band in ^{78}Ni consistent with data

Rotational bands in odd-mass neon
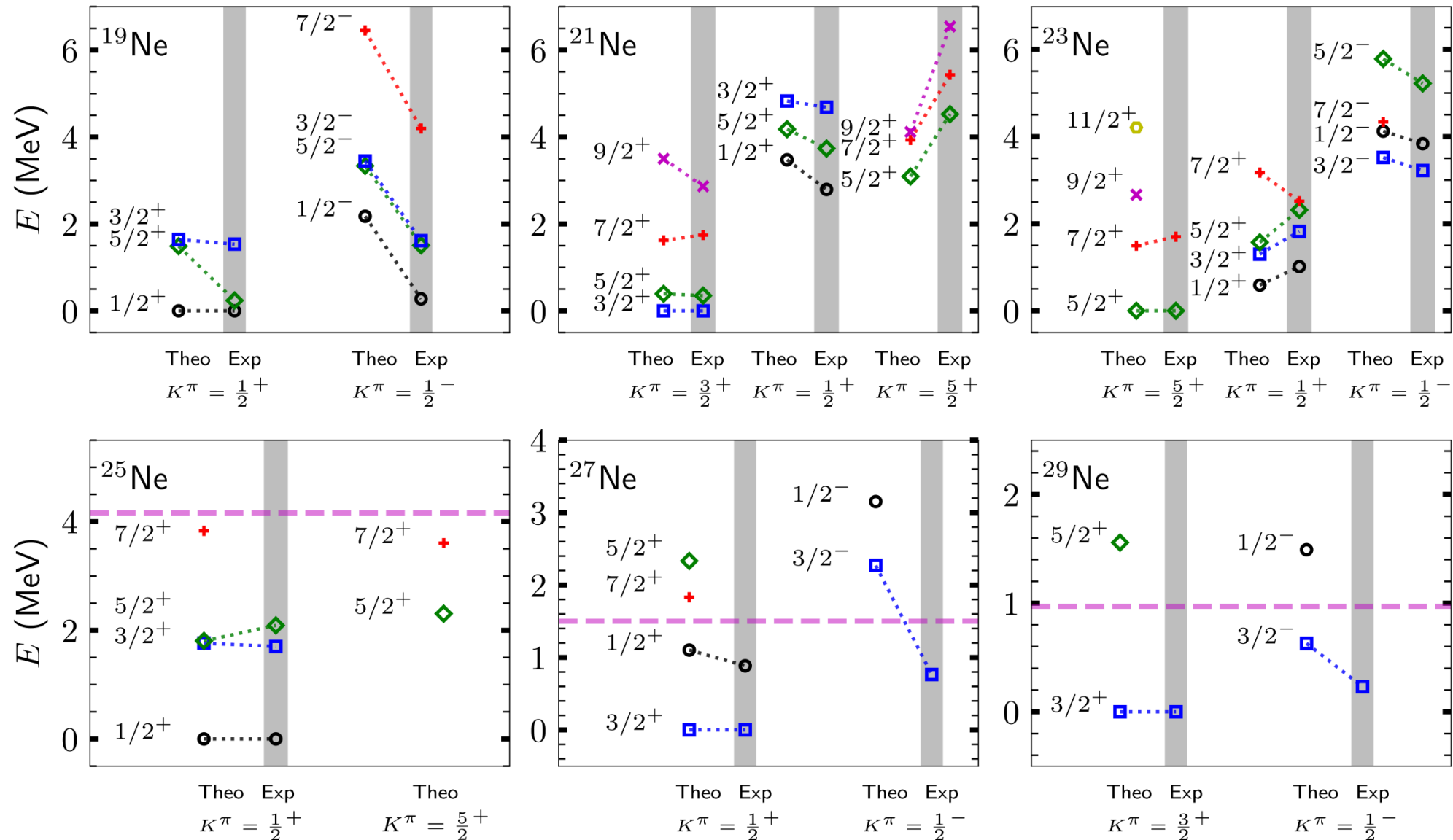
Symmetry restored coupled-cluster theory

Projection after variation (PAV):

$$E^{(J)} = \frac{\langle \widetilde{\Psi} | P_J H | \Psi \rangle}{\langle \widetilde{\Psi} | P_J | \Psi \rangle}$$

Right coupled-cluster state: $|\Psi\rangle = e^T |\Phi_0\rangle$

Left state is parametrized differently:

$$\langle \widetilde{\Psi} | = \langle \Phi_0 | (1 + \Lambda) e^{-T}$$

Bi-variational

$$P_J = \frac{1}{2} \int_0^\pi d\beta \sin(\beta) d_{00}^J(\beta) R(\beta)$$

Image credit: Wikimedia Commons

For axial symmetry around the z-axis the rotation operator is:

$$R(\beta) \equiv e^{i\beta J_y}$$

Symmetry restored coupled-cluster theory

The kernels can be evaluated by using Thouless theorem:

$$\langle\Phi_0|R(\beta) = \langle\Phi_0|R(\beta)|\Phi_0\rangle\langle\Phi_0|e^{V_1(\beta)}$$

$$\mathcal{H}(\beta) = \langle\Phi|\overline{R}(\beta)|\Phi\rangle\langle\Phi|Z(\beta)\widetilde{H}(\beta)e^{V(\beta)}e^{T_2}|\Phi\rangle$$

$$\mathcal{N}(\beta) = \langle\Phi|\overline{R}(\beta)|\Phi\rangle\langle\Phi|Z(\beta)e^{V(\beta)}e^{T_2}|\Phi\rangle$$

Similarity transformed rotation operator and Hamiltonian:

$$e^{V(\beta)}e^{T_2}|\Phi\rangle = e^{W_0(\beta)+W_1(\beta)+W_2(\beta)+\cdots}|\Phi\rangle$$

$$\overline{R}(\beta) = e^{-T_1}R(\beta)e^{T_1}$$

$$\widetilde{H}(\beta) = e^{V_1(\beta)}\overline{H}e^{-V_1(\beta)}$$

- Does not truncate
- How to evaluate the disentangled amplitudes?

[Qiu et al, J. Chem. Phys. 147, 064111 (2017)]

# Solving for the disentangled amplitudes [Qiu et al]

Approximate:
$$e^{V(\beta)}e^{T_2}|\Phi\rangle \approx e^{W_0(\beta)+W_1(\beta)+W_2(\beta)}|\Phi\rangle$$

Taking the derivative with respect to β leads to a set of ODEs with initial conditions:
$$W_0(\beta = 0) = W_1(\beta = 0) = 0, W_2(\beta = 0) = T_2$$
[Qiu et al, J. Chem. Phys. 147, 064111 (2017)]

- Approximate restoration of symmetries
- Can lead to stiffness as $dV(\beta)/d(\beta)$ might be large for $\langle\Phi|R(\beta)|\Phi\rangle \approx 0$.
- The truncation at W_2 might lead to loss of accuracy at larger angles
- Kernels are not symmetric around $\beta = \frac{\pi}{2}$
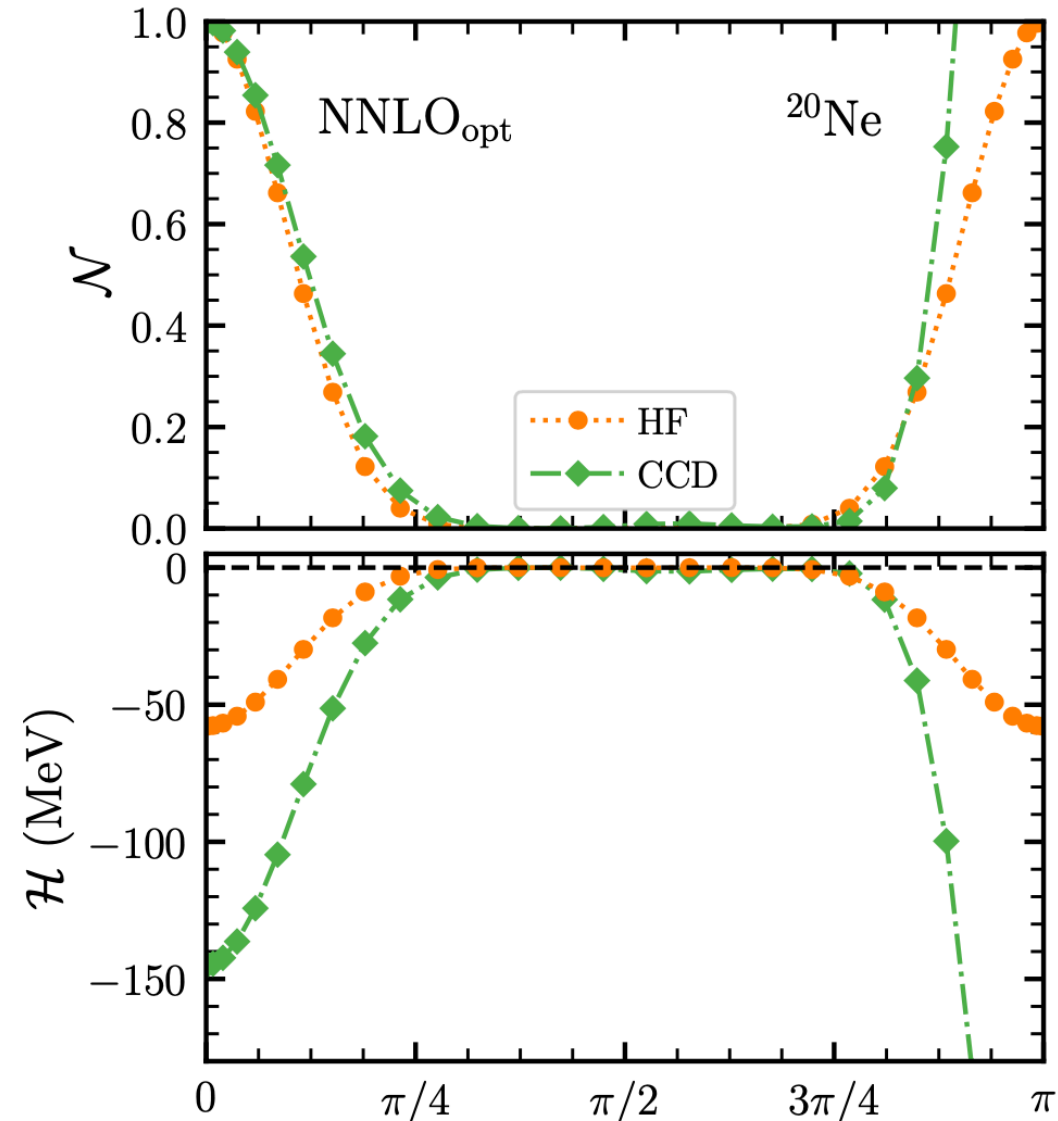
New approach to solve for disentangled amplitudes

We write: $$e^{\lambda V} e^{T_2} |\Phi\rangle \approx e^{W_0(\lambda) + W_1(\lambda) + W_2(\lambda)} |\Phi\rangle$$

Taking the derivative with respect to λ for fixed β leads to a new set of ODEs with initial conditions: $W_n(\lambda = 0) = T_n$

- Approximate restoration of symmetries
- Significantly improves stability of ODEs
- Kernels are fully symmetric around $\beta = \frac{\pi}{2}$

Zhonghao Sun, A. Ekstrom, C. Forssen,
G. Hagen. G. R. Jansen, T. Papenbrock (2024)
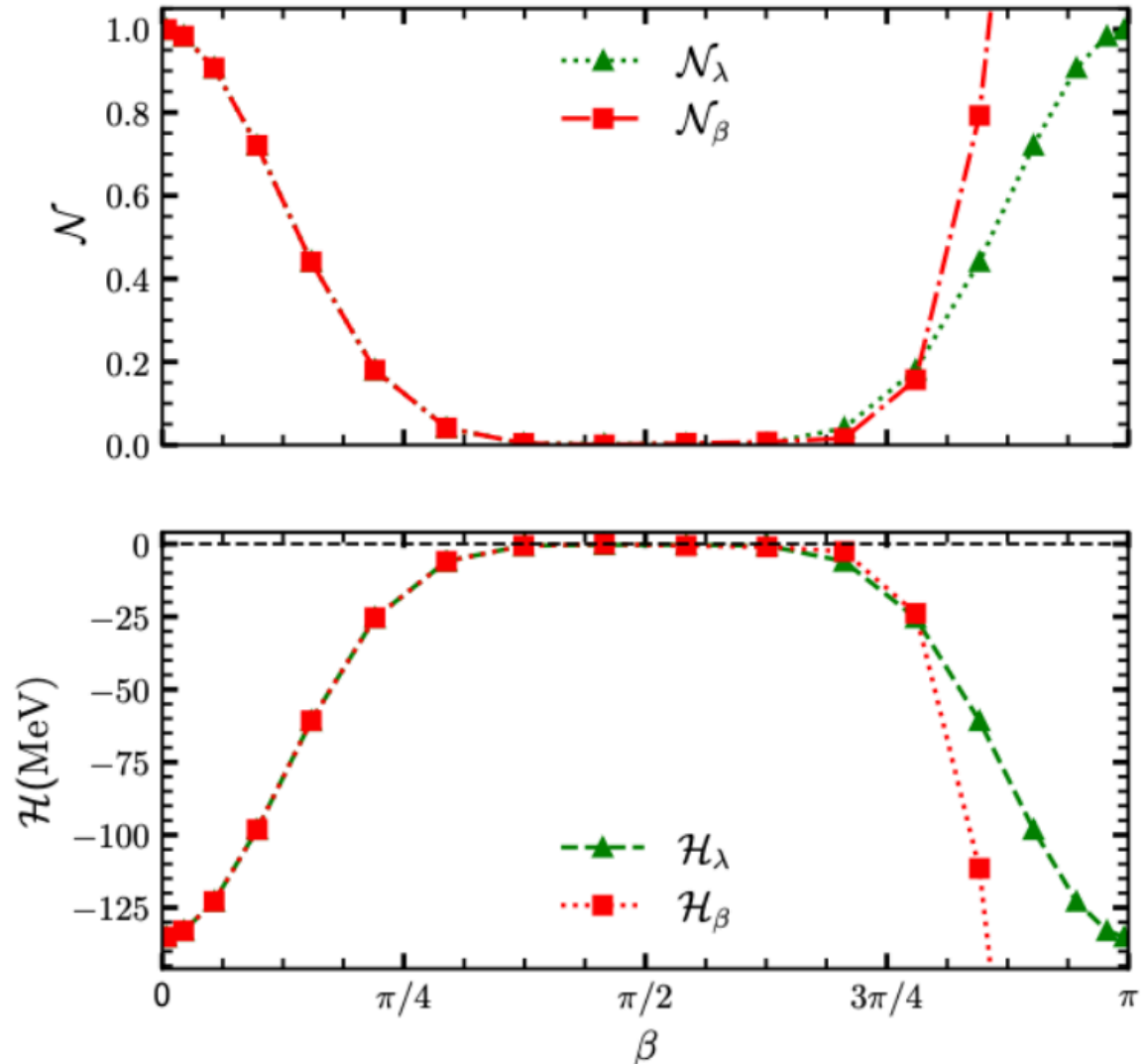
Electromagnetic transitions

$$B(E2,\downarrow) \equiv |\langle 0^+ ||Q_2||2^+\rangle|^2$$

$$B(E2,\downarrow) = \frac{\langle\widetilde{\Psi}|P_0 Q_{20} P_2|\Psi\rangle\langle\widetilde{\Psi}|P_2 Q_{20} P_0|\Psi\rangle}{\langle\widetilde{\Psi}|P_0|\Psi\rangle\langle\widetilde{\Psi}|P_2|\Psi\rangle}$$

Recall the left and right coupled-cluster states:

$$\langle\widetilde{\Psi}| \equiv \langle\Phi_0|(1+\Lambda)e^{-T} \qquad |\Psi\rangle \equiv e^T|\Phi_0\rangle$$

Benchmarking projected coupled-cluster in ^{20}Ne
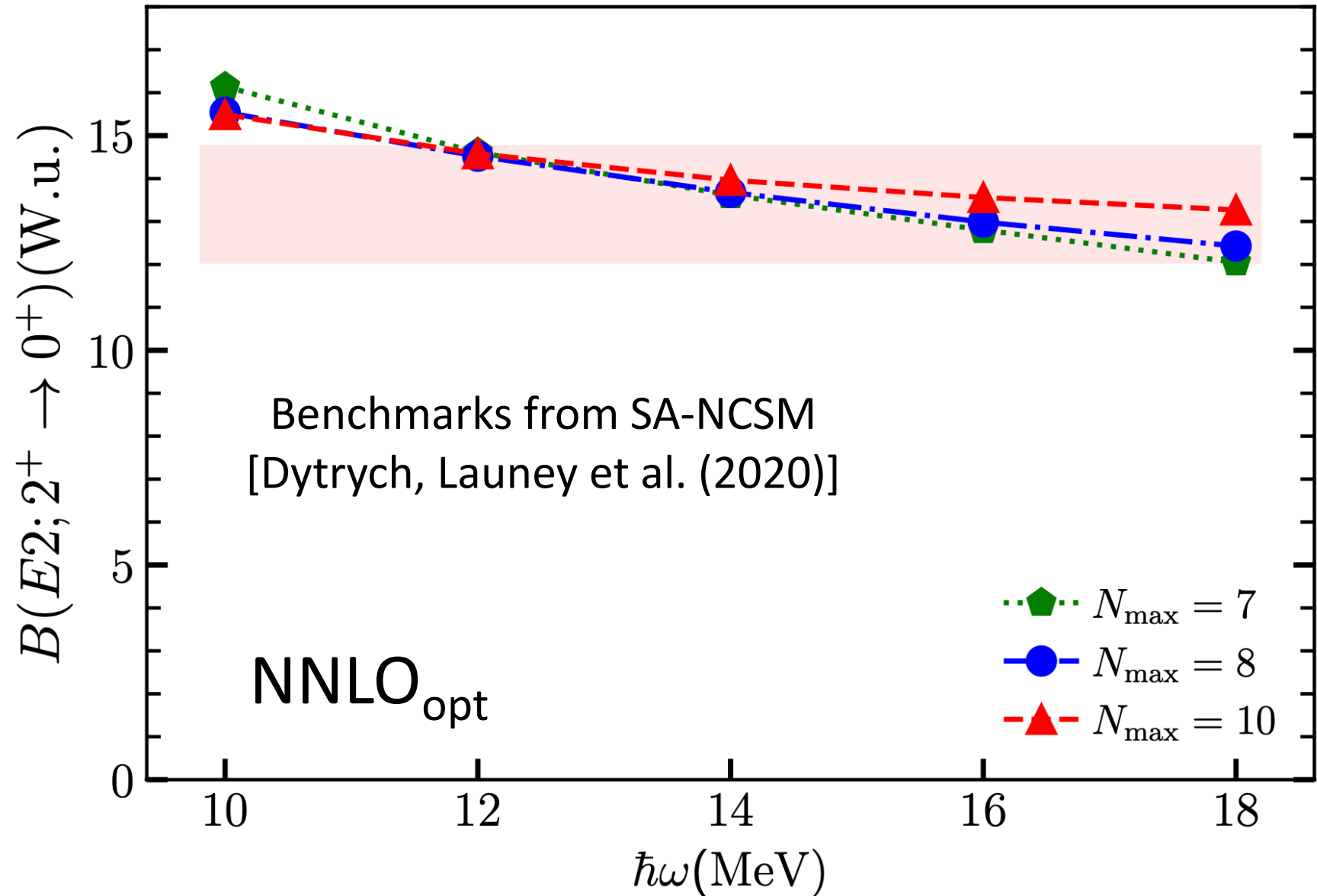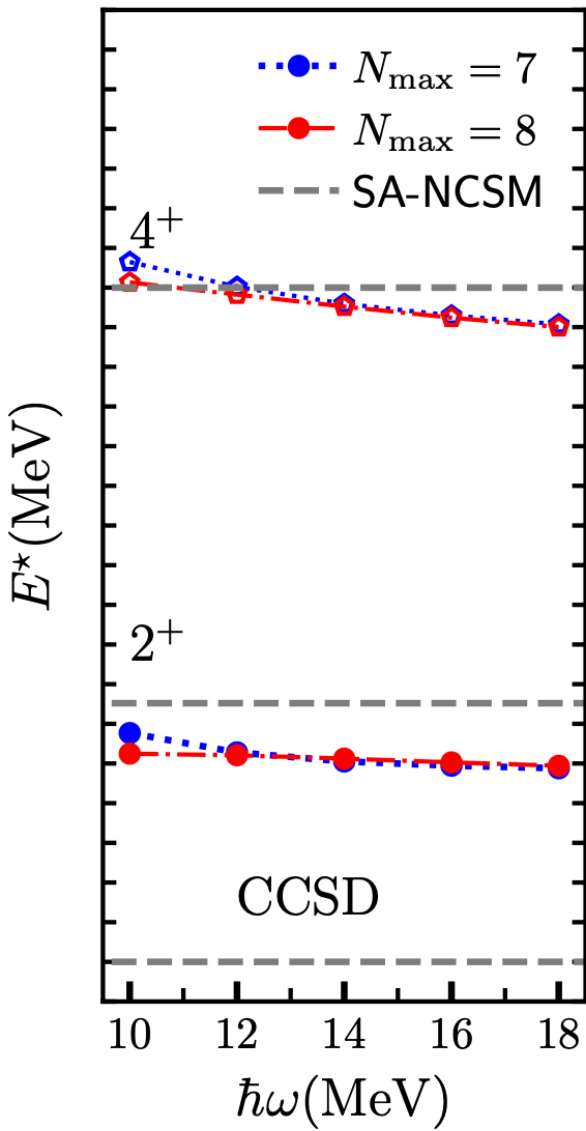
Ground-state energies of neon isotopes

1.8/2.0(EM)

$N_{max} = 12$, hw = 14MeV

HF
CCSD
CCSDT1
Exp

ΔE

$\sim 10\% \Delta E$

E(MeV)

^{20}Ne ^{22}Ne ^{24}Ne ^{26}Ne ^{28}Ne ^{30}Ne ^{32}Ne ^{34}Ne
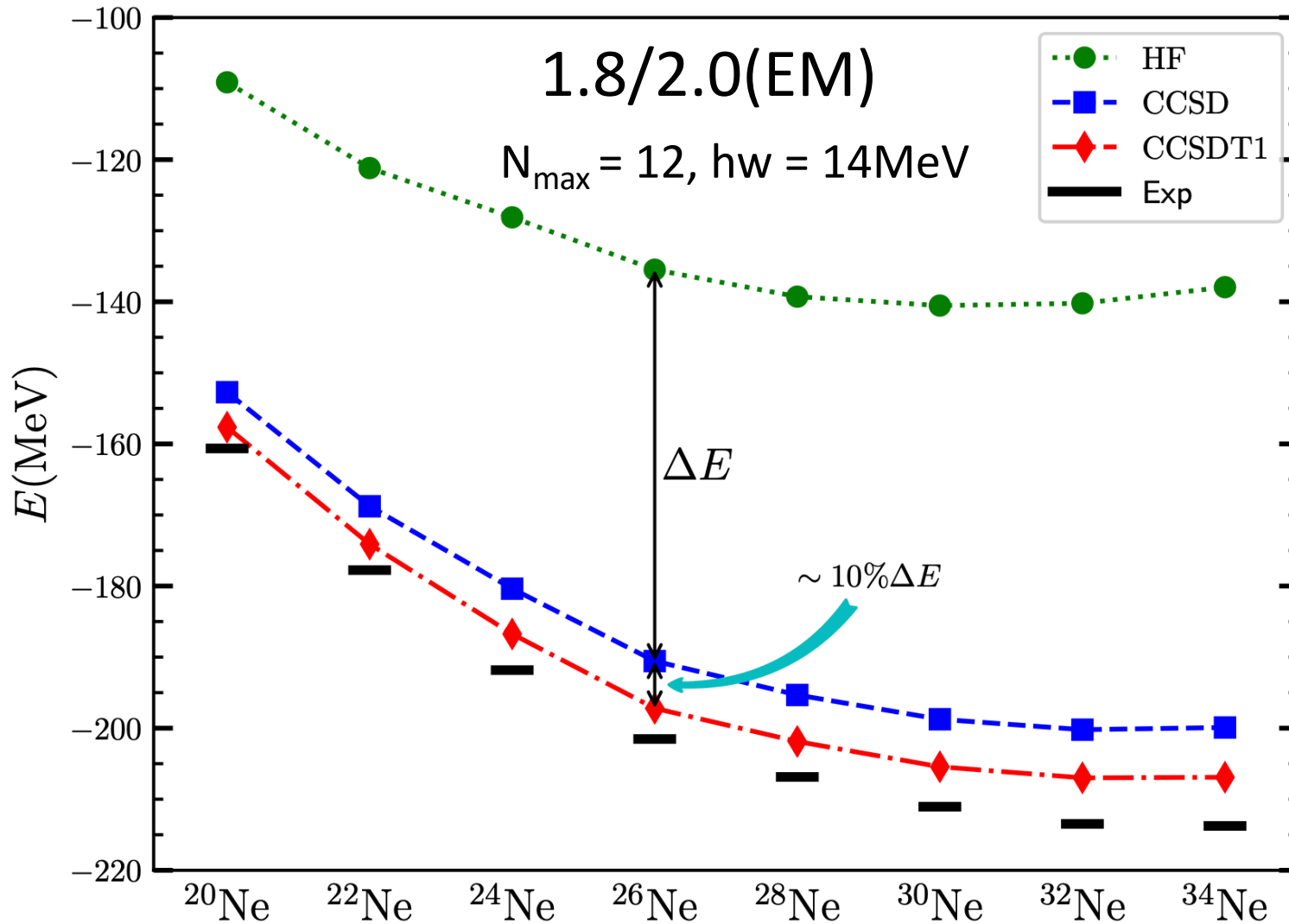
- Use natural orbitals for better convergence of triples excitations
- Computed binding energies overall in good agreement
- Triples excitations yield ~10% of CCSD correlation energy

Zhonghao Sun, A. Ekstrom, C. Forssen, G. Hagen. G. R. Jansen, T. Papenbrock (2024)

Shape co-existence in ³²Mg

(a) ³²Mg

Deformed

Spherical

N_{max}

6, 8, 10, 12

$E_{HF}(MeV)$

$q_{20}(fm^2)$

(b) N_{max}

$E(MeV)$

Spherical, CCSD — Deformed, CCSD
Spherical, CCSD+(T) — Deformed, CCSD+(T)

Exp

(c) $E^\star(MeV)$

4^+
2^+
0^+
4^+
2^+
0^+
4^+
2^+
0^+

Spherical Deformed Expt

Zhonghao Sun, A. Ekstrom, C. Forssen, G. Hagen. G. R. Jansen, T. Papenbrock (2024)
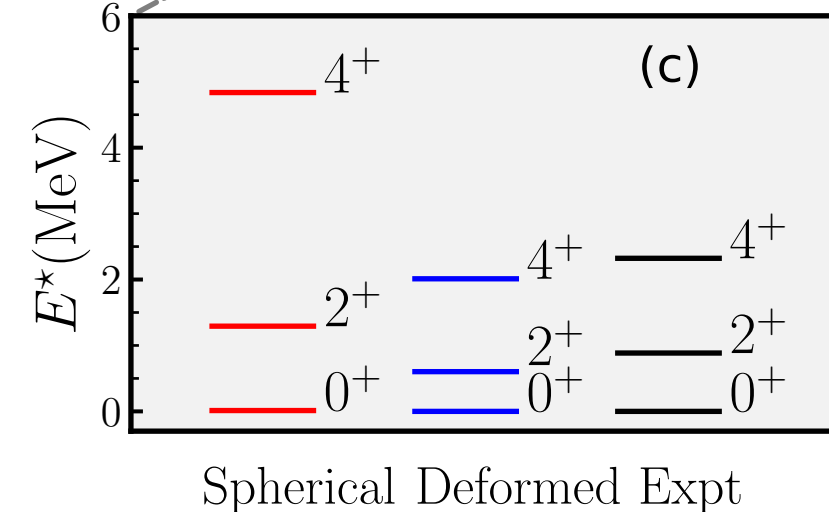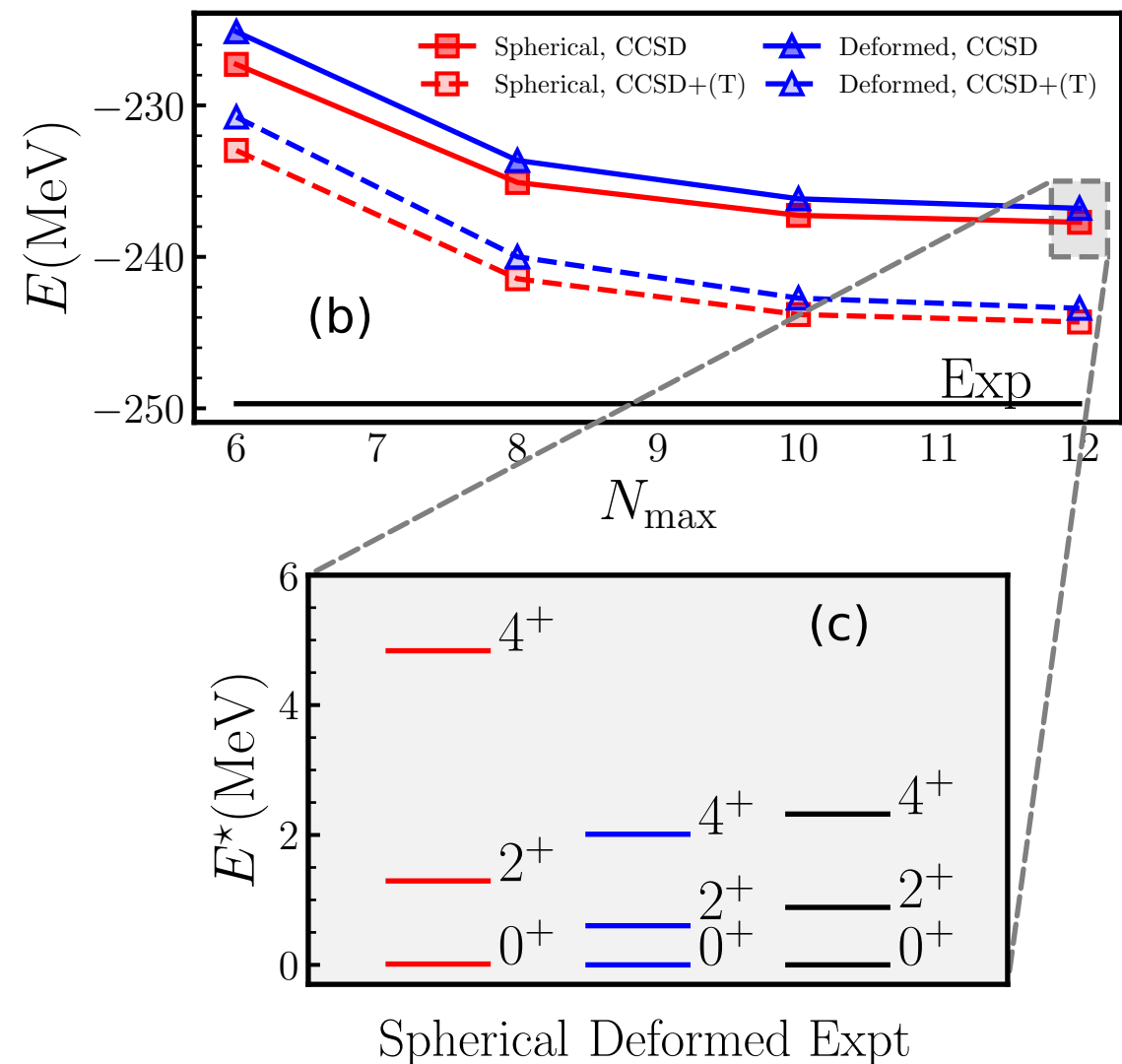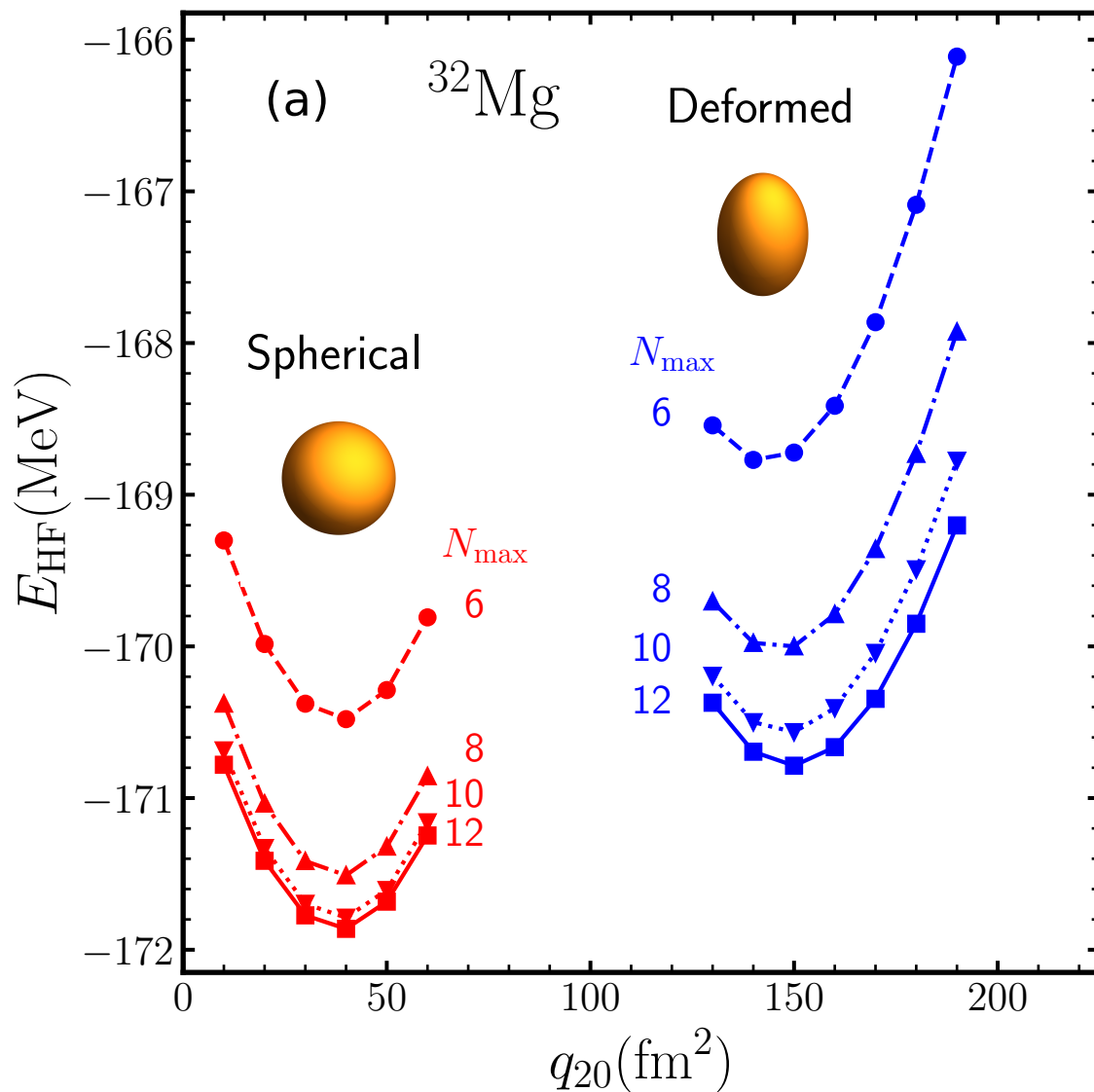
# Onset of deformation and shape co-existence along N = 20

Shape co-existence in ^{32}Mg
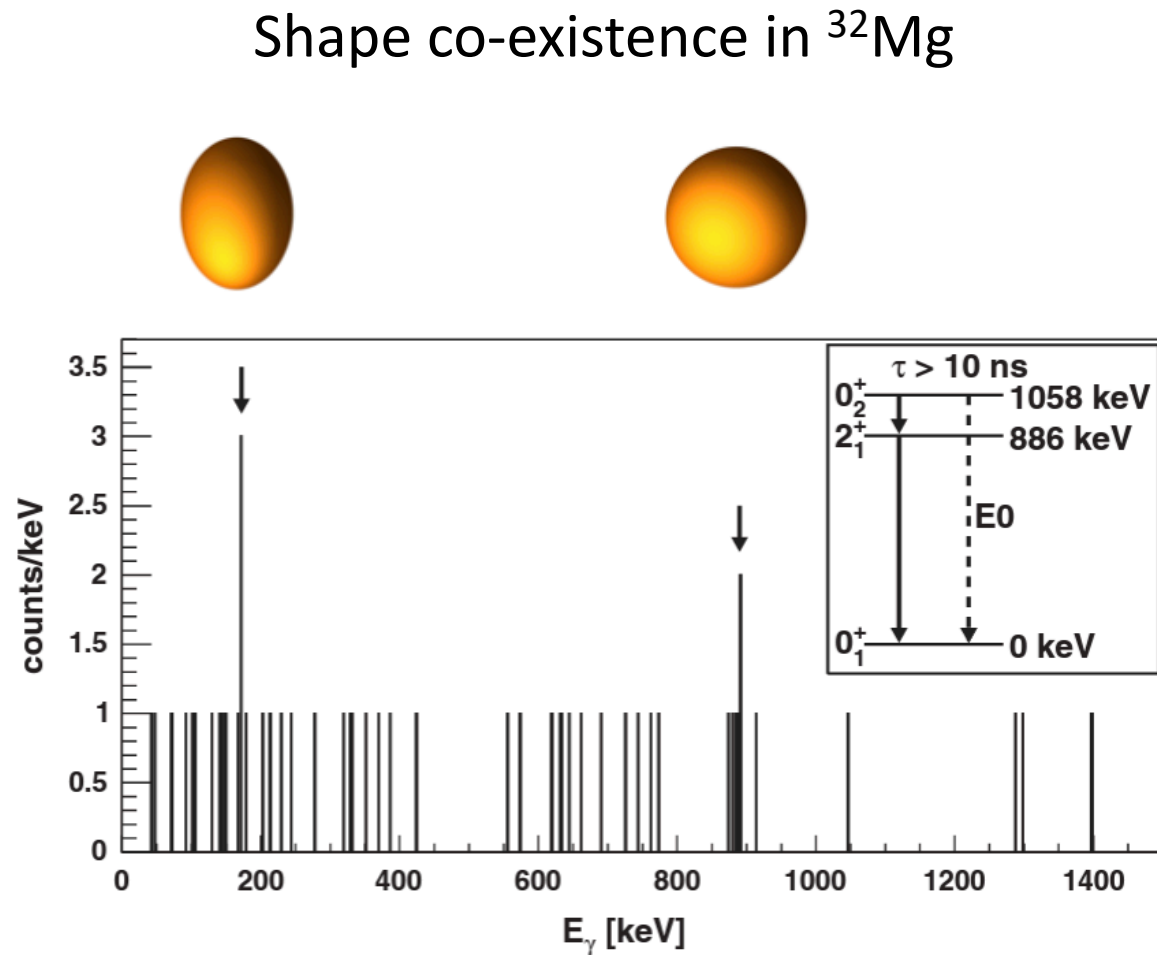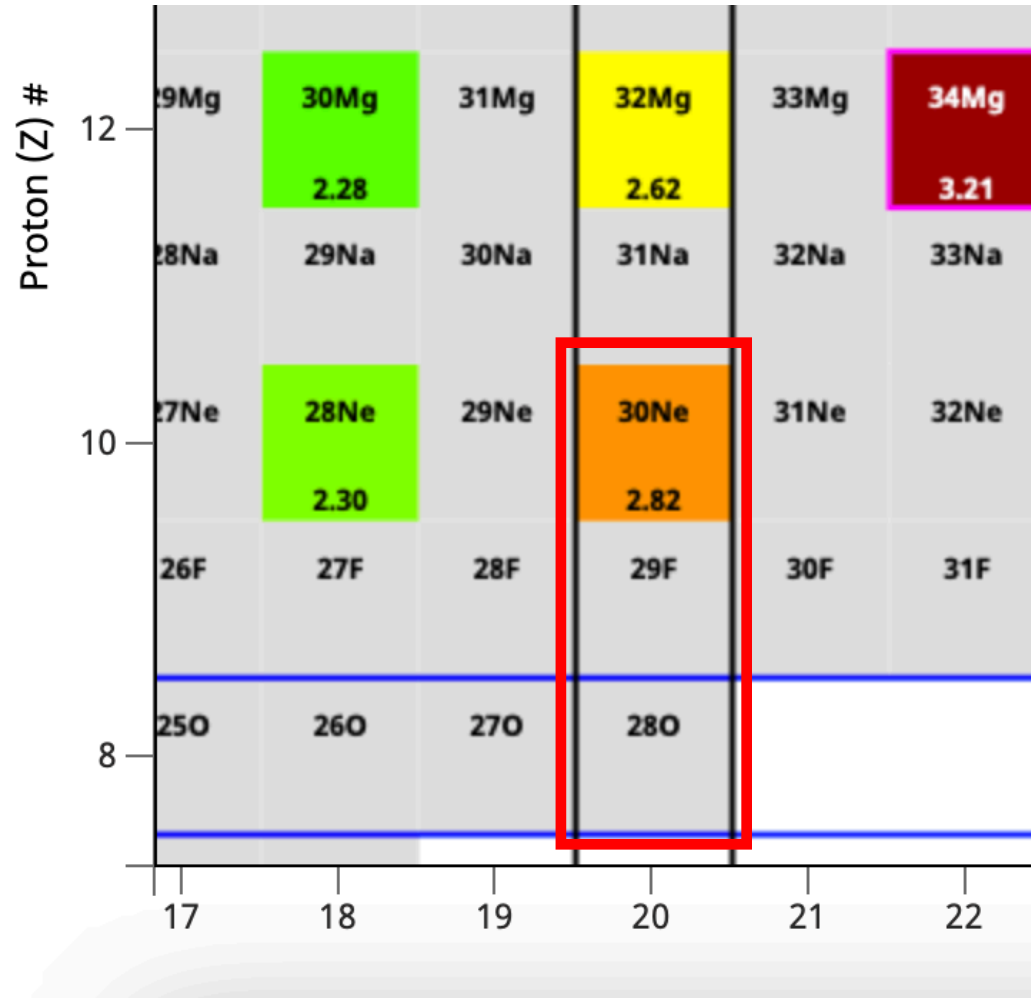
K. Wimmer et al, PRL (2010)

Coupled-cluster method

$$\Psi = e^T |\Phi\rangle$$

$$T = T_1 + T_2 + \ldots$$

$$T_1 = \sum_{ia} t_i^a a_a^\dagger a_i \quad T_2 = \frac{1}{4} \sum_{ijab} t_{ij}^{ab} a_a^\dagger a_b^\dagger a_j a_i$$

- ☺ Scales gently (polynomial) with increasing system size
- ☺ Truncation is only approximation
- ☺ Fulfills a bi-variational principle
- ☺ A lot of freedom in the choice of reference state (spherical, deformed, pairing,…)

$$\bar{H}_{\mathrm{CCSD}} = \begin{pmatrix} E_{\mathrm{CCSD}} & \bar{H}_{0S} & \bar{H}_{0D} \\ 0 & \bar{H}_{SS} & \bar{H}_{SD} \\ 0 & \bar{H}_{DS} & \bar{H}_{DD} \end{pmatrix} \begin{matrix} \mathrm{0p0h} \\ \mathrm{1p1h} \\ \mathrm{2p2h} \end{matrix}$$

(columns labeled 0p0h, 1p1h, 2p2h)

$$E = \langle \Phi | \bar{H} | \Phi \rangle$$
$$0 = \langle \Phi_i^a | \bar{H} | \Phi \rangle$$
$$0 = \langle \Phi_{ij}^{ab} | \bar{H} | \Phi \rangle$$
$$\bar{H} \equiv e^{-T} H e^T = \left(H e^T \right)_c = \left(H + HT_1 + HT_2 + \frac{1}{2} HT_1^2 + \ldots \right)_c$$

CCSD generates similarity transformed Hamiltonian with no 1p-1h and no 2p-2h excitations

Correlations are *exponentiated* 1p-1h and 2p-2h excitations. Part of Ap-Ah excitations included!
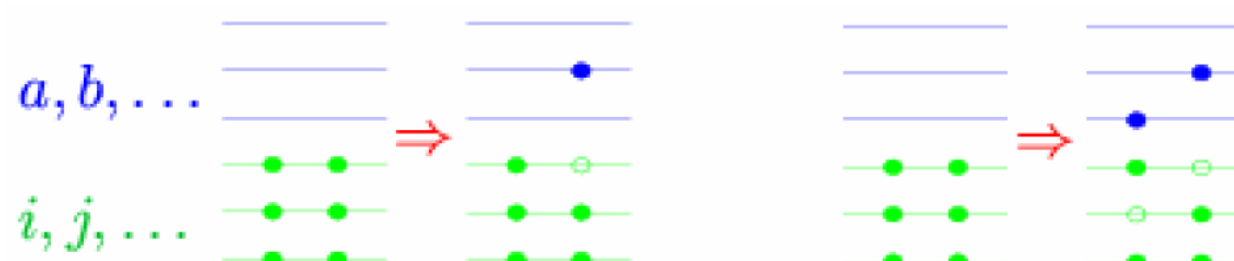
Cross-validation of projected HF emulator

400 cross-validation points 10% around Delta-GO(394)

Total energy

^{32}Ne

R42 ratio
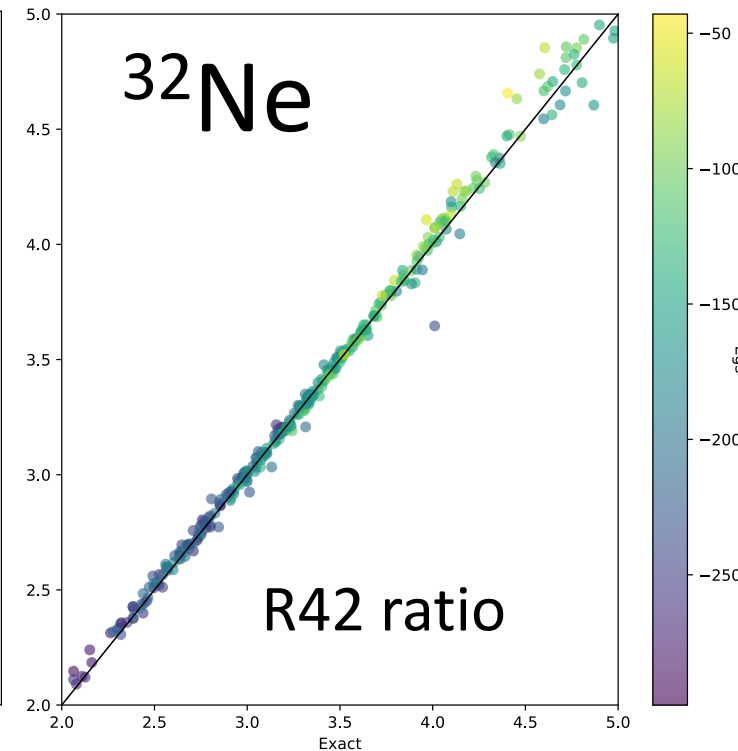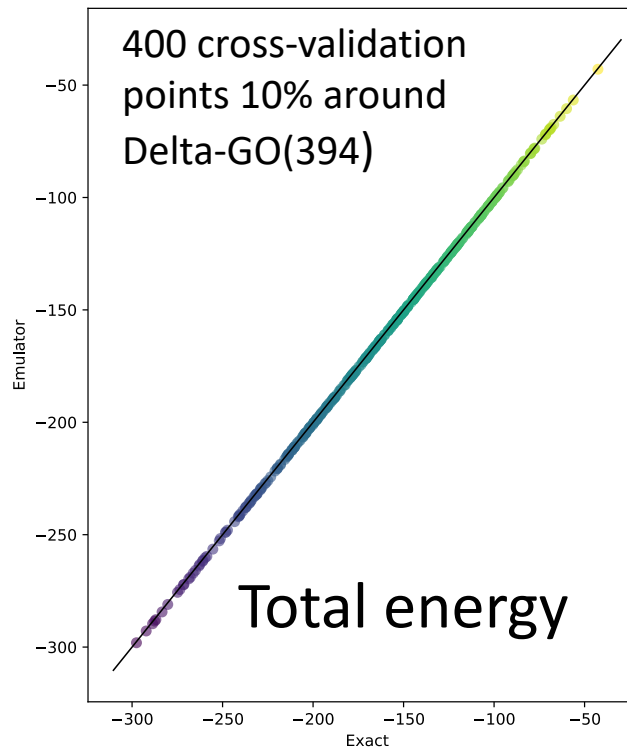
Accuracy of R42 emulators as measured by the difference with respect to 400 exact Hartree-Fock calculations

The standard deviation of the differences indicates a relative precision of 1%

The emulated energies are accurate on the 10 keV level
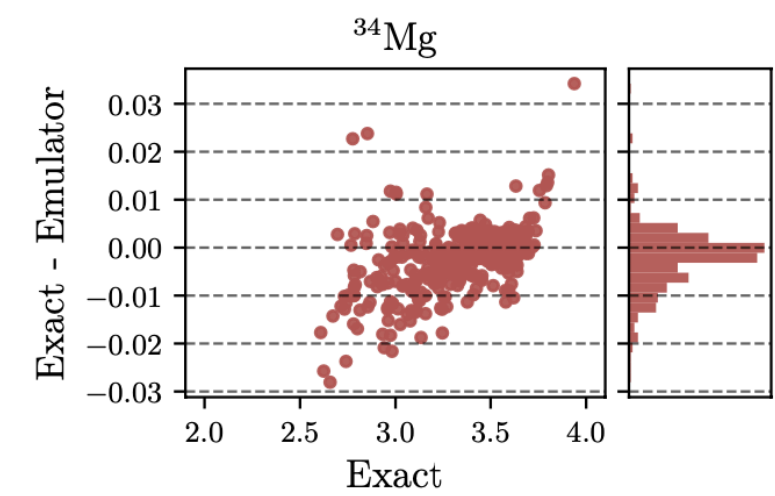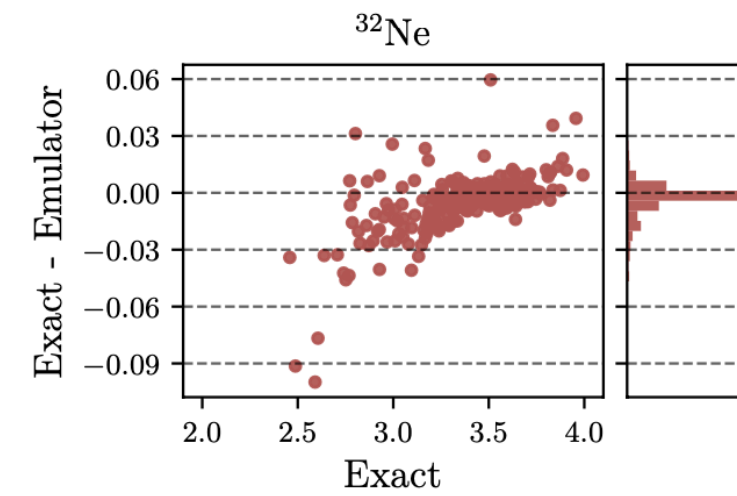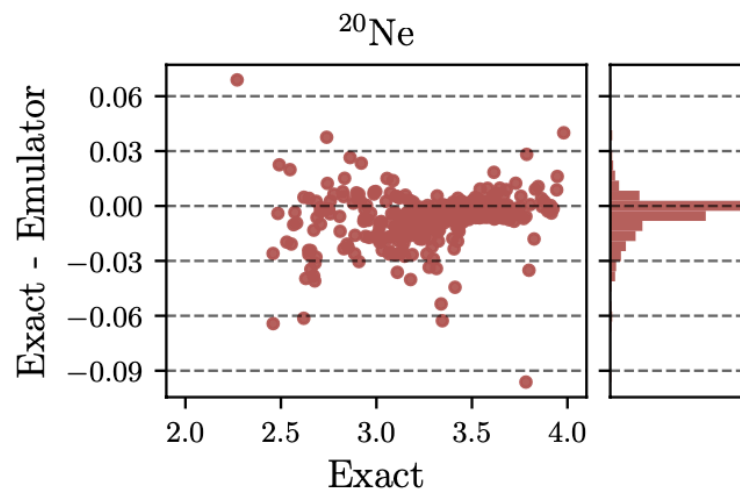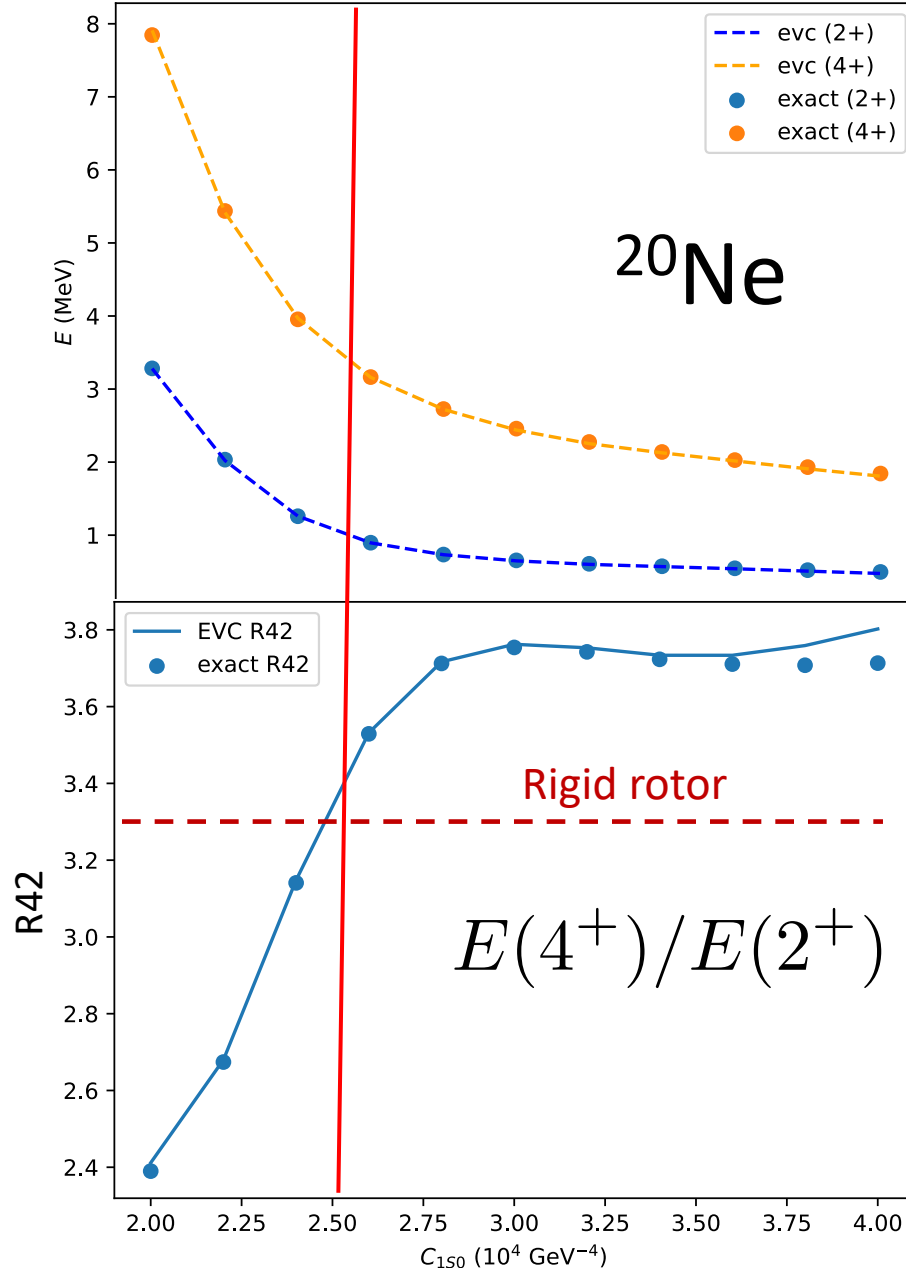
^{20}Ne

^{32}Ne

^{34}Mg

Linking deformation to nuclear forces

^{20}Ne

Rigid rotor

$E(4^+)/E(2^+)$

C_{1S0} (10^4 GeV^{-4})

2N Force

3N Force

LO $(Q/\Lambda_\chi)^0$

NLO $(Q/\Lambda_\chi)^2$

Vary only C_{1S_0}

NNLO $(Q/\Lambda_\chi)^3$

- Constructed accurate and efficient emulator of projected HF using 68 training vectors
- Training points obtained by using Latin Hypercube sampling within 20% of original low-energy constants

Deformation in neutron-rich magnesium
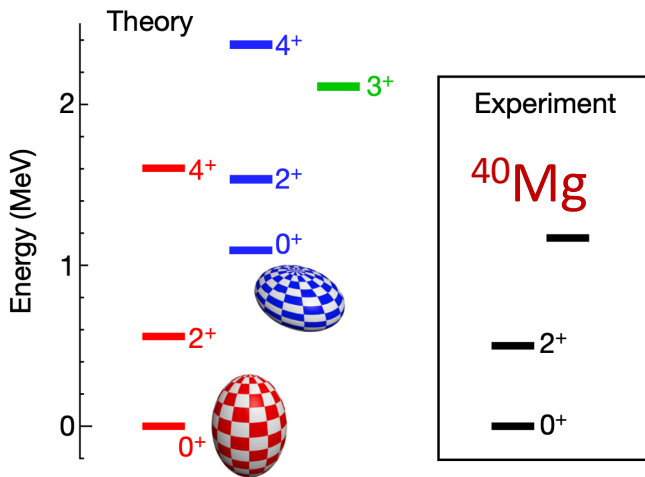
Crawford et al. PRL 122, 052501 (2019)

Tsunuda et al, Nature 587, 66 (2020)

Ikuko Hamamoto, Phys. Rev. C **93**, 054328 (2016)
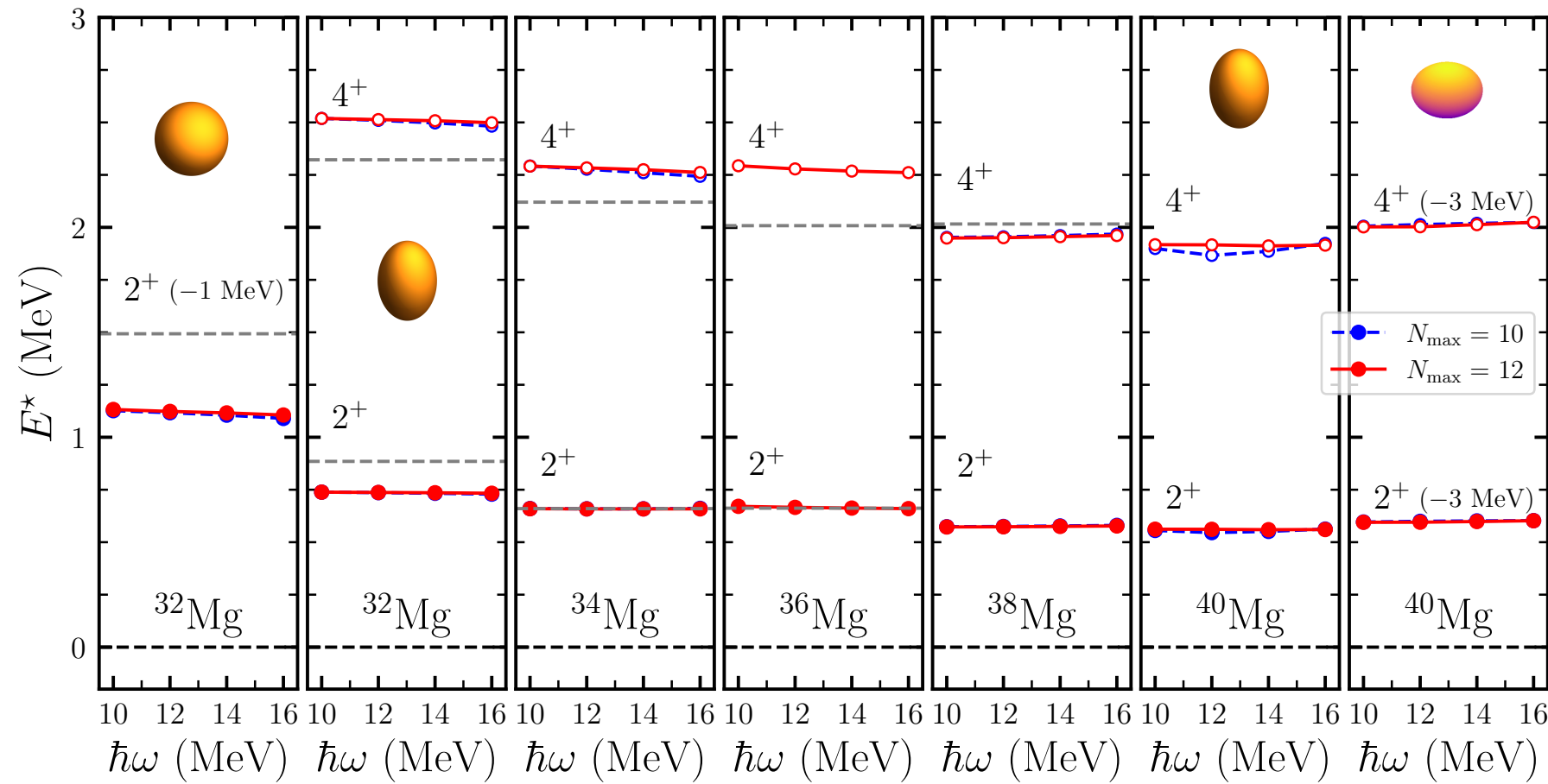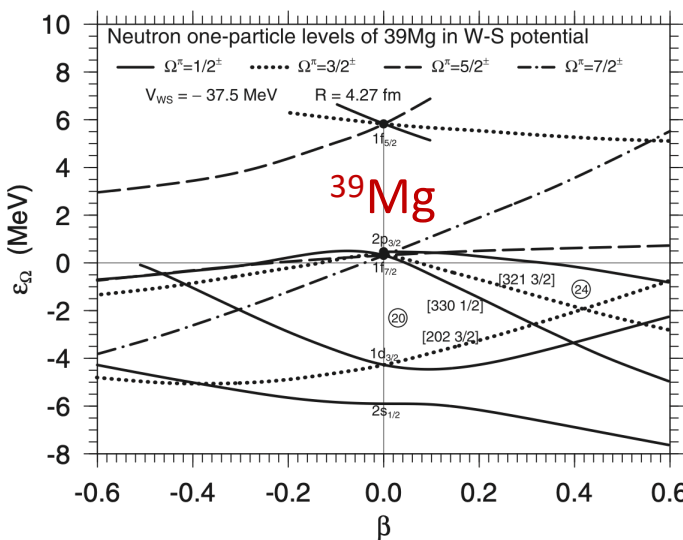
- Rotational structure in good agreement with experiment
- Indications of shape co-existence in ^{40}Mg
- Find oblate band in ^{40}Mg 2-3MeV above the prolate band

Emulating rotational structure of ^{20}Ne

Varying only one parameter: C_{1S_0}

Zhonghao Sun, Andreas Ekström, Christian Forssén, G. Hagen, G. R. Jansen, T. Papenbrock (2024)